imec

A dynamic addressing architecture for multi-electrode arrays towards ultra-high-density DNA synthesis

2025-06-19 **Kherim Willems**, Senne Fransen *et al.*

SORBONNE UNIVERSITÉ BIOMEMORY Sustainable Storage Solutions DNA DATA STORAGE ALLIANCE SNIA

IMEC IS A WORLD LEADING RESEARCH CENTER FOCUSING ON SEMICONDUCTOR TECHNOLOGY, DESIGN AND APPLICATION

—

BRIDGING THE GAP BETWEEN ACADEMIA AND INDUSTRY.

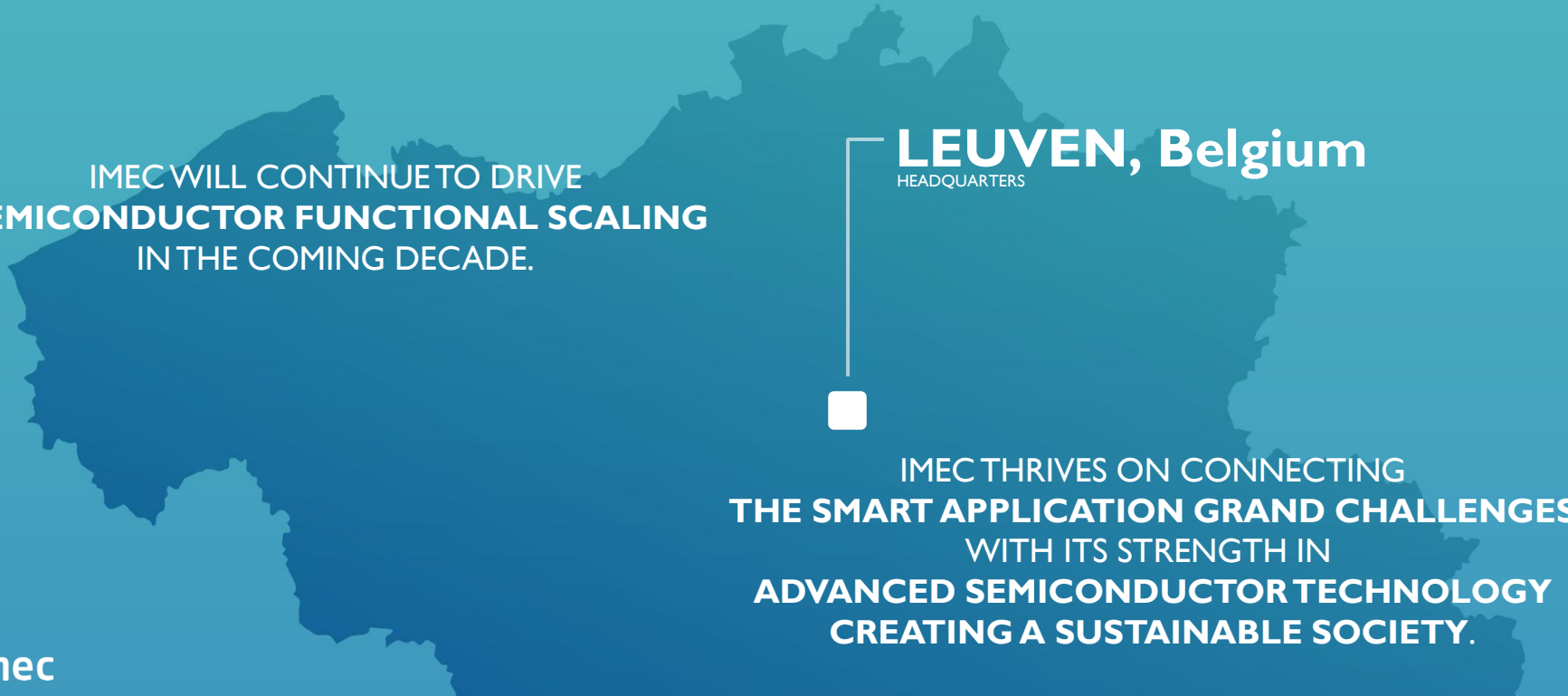

IMEC WILL CONTINUE TO DRIVE
SEMICONDUCTOR FUNCTIONAL SCALING
IN THE COMING DECADE.

LEUVEN, Belgium
HEADQUARTERS

IMEC THRIVES ON CONNECTING
THE SMART APPLICATION GRAND CHALLENGES
WITH ITS STRENGTH IN
ADVANCED SEMICONDUCTOR TECHNOLOGY
CREATING A SUSTAINABLE SOCIETY.

imec

World-class infrastructure

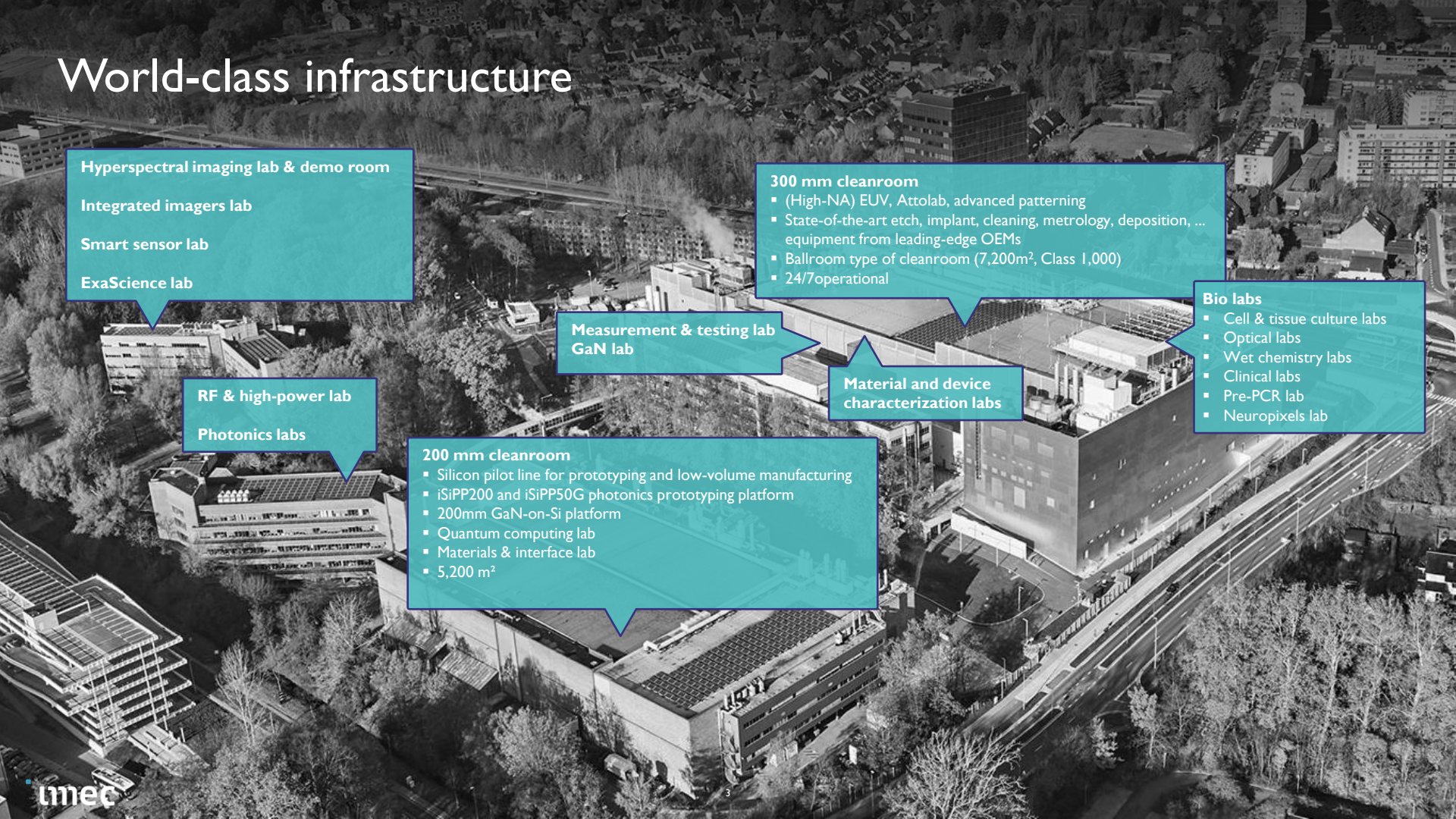

The **cost** and **throughput** gaps facing the **"write"** aspect of DNA-based data storage span **many orders of magnitude**

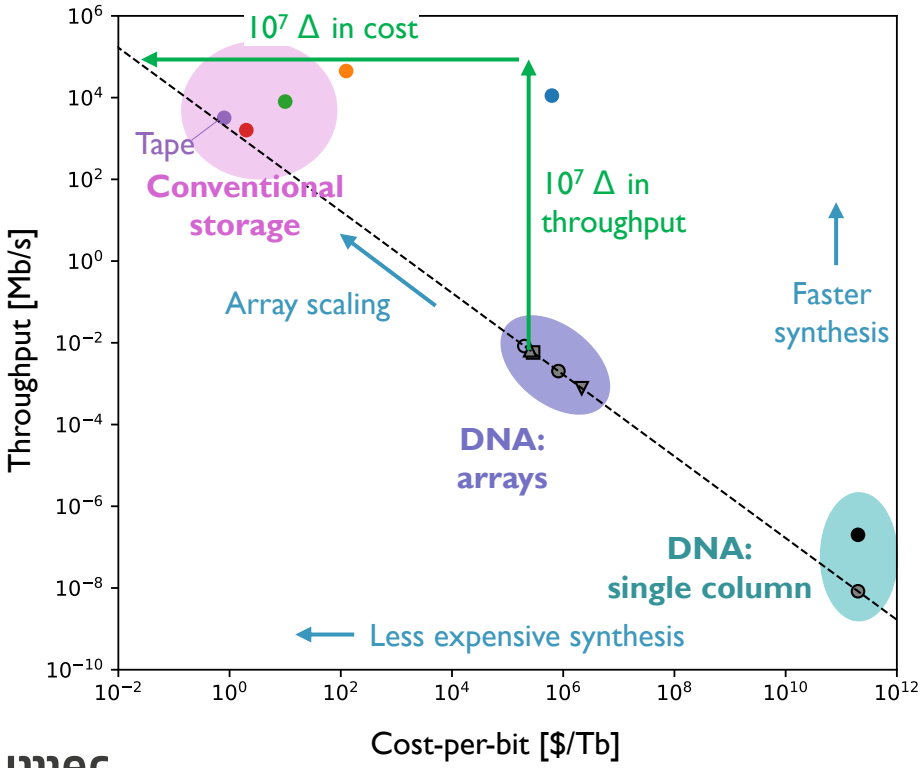

- Both **cost and throughput** require at least **1E7x improvement** to **surpass tape**, the current SoA
- Both can be tackled at the same time through **density scaling** of the synthesis sites
- However, for archival storage the **total cost-of-ownership** (TCO) is more relevant than the raw write-cost

DNA synthesis can be **multiplexed** on micro-electrode arrays using **localized quinone electrochemistry** to perform the **deblocking**

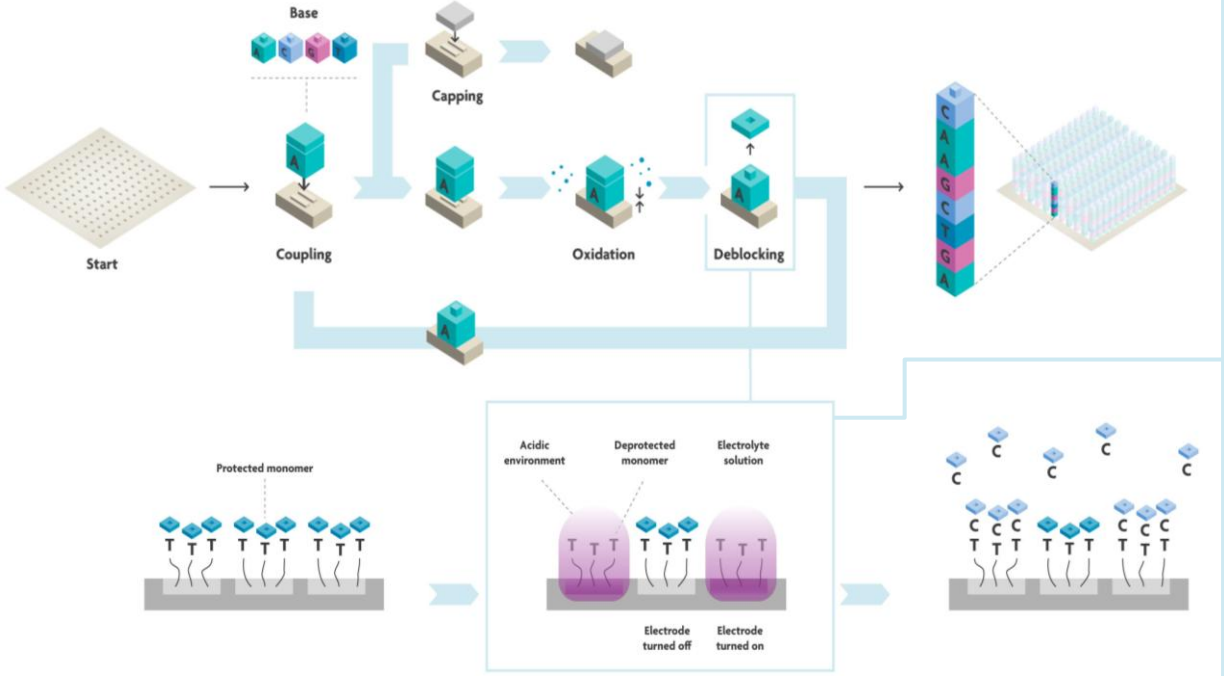

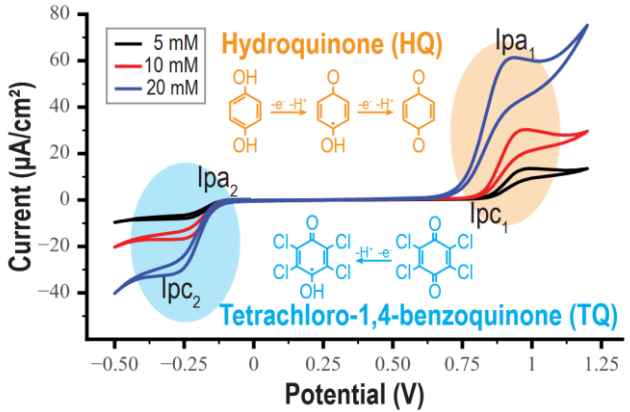

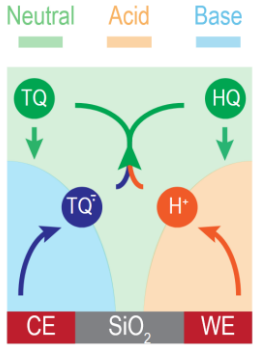

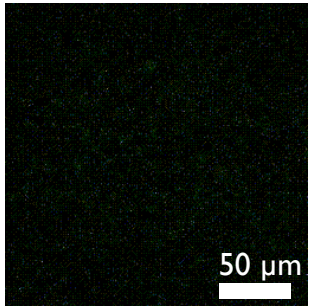

Ghadami et al., 2022 IEEE Symposium on VLSI Technology and Circuits

Underneath each electrode sits a CMOS-based **switch** that must be as **small** as possible while remaining **application-compatible**

HELIX: 160K sites on ~0.7×0.9 mm² (1.8×2.2 µm²)

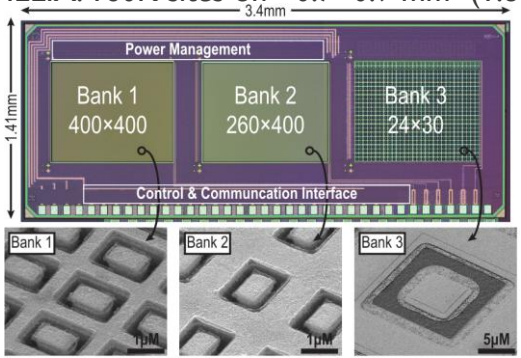

Ghadami et al., 2022 IEEE Symposium on VLSI Technology and Circuits

Twist: 128M sites on ~20×20 mm² (1×2 µm²)

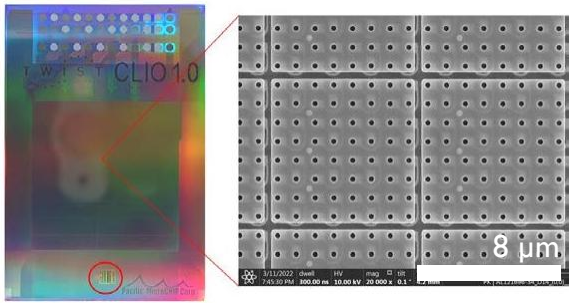

SRAM (6T): both a memory and switch

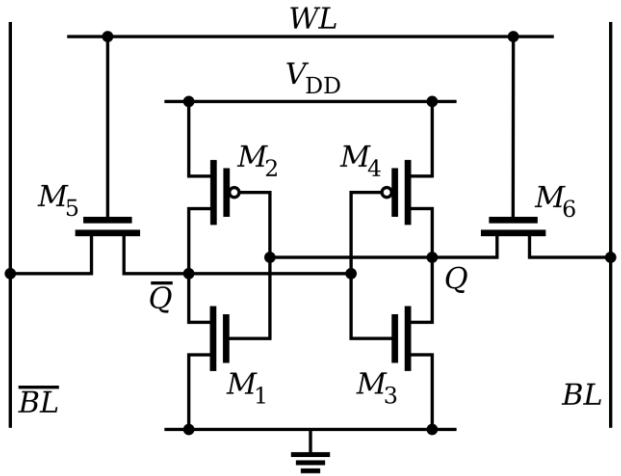

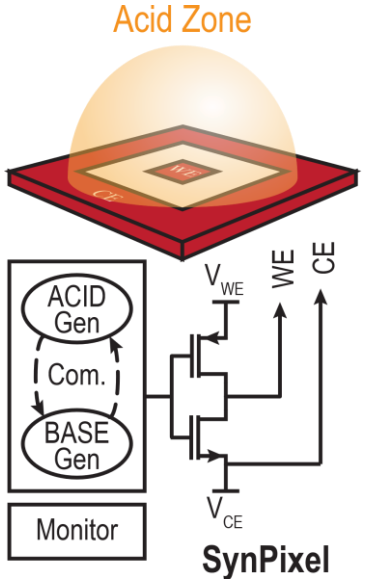

- Markowitz, "Biology Is All You Need", Supercomputing 22

For a similar technology node, **dynamic** memories require **20× less area per bit cell** compared to **static** memories

SRAM "6T" bit cell

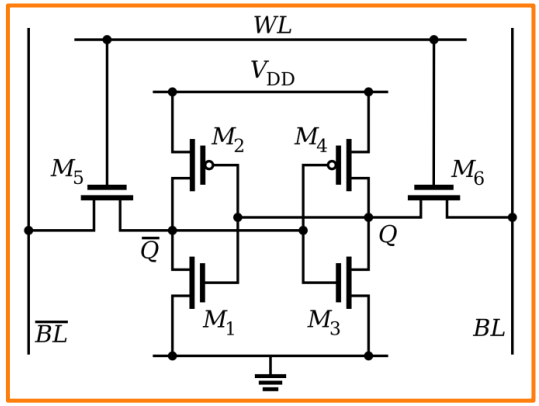

DRAM "1T1C" bit cell

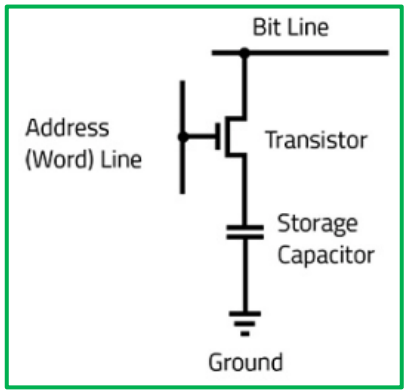

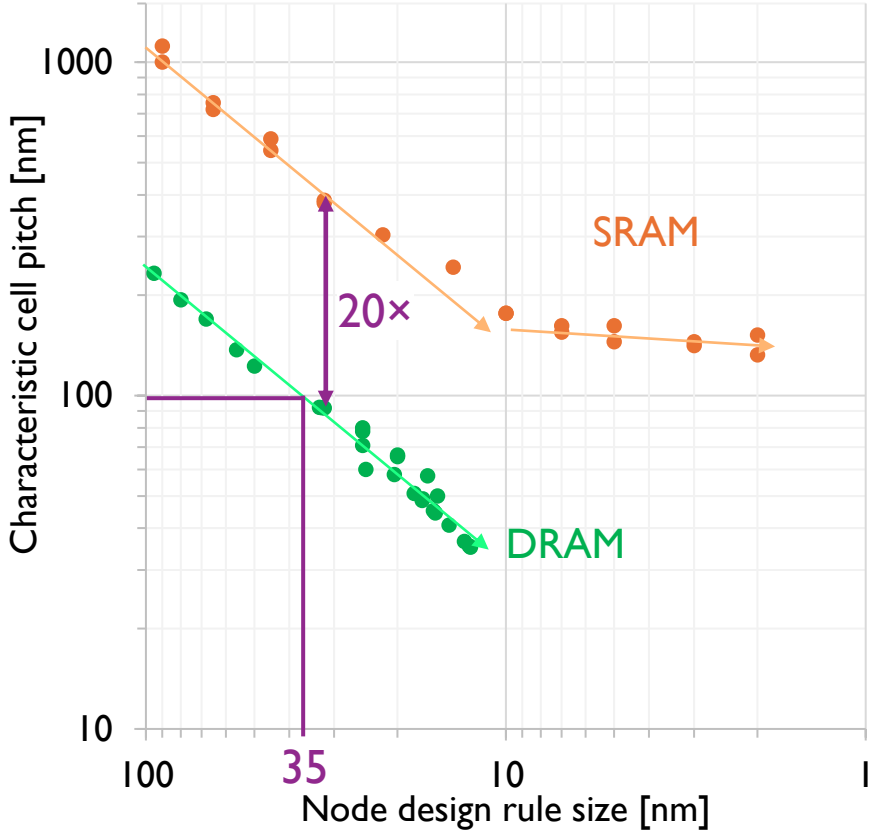

imec

Dynamic addressing can drive electrochemical **deblocking**, but we must determine the **minimal duty cycle** that can sustain it

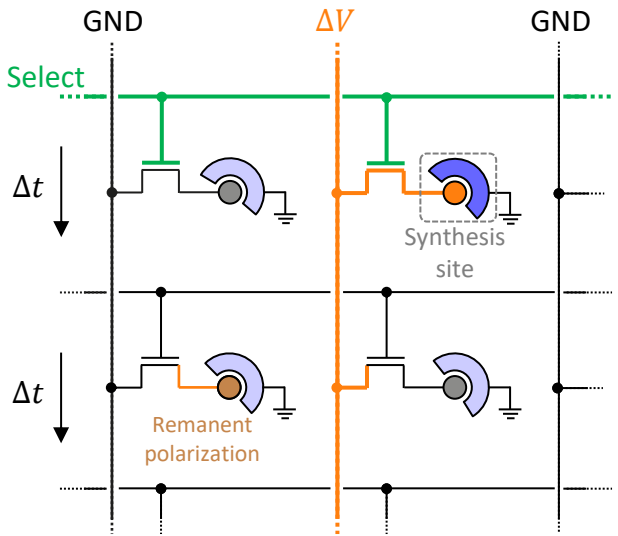

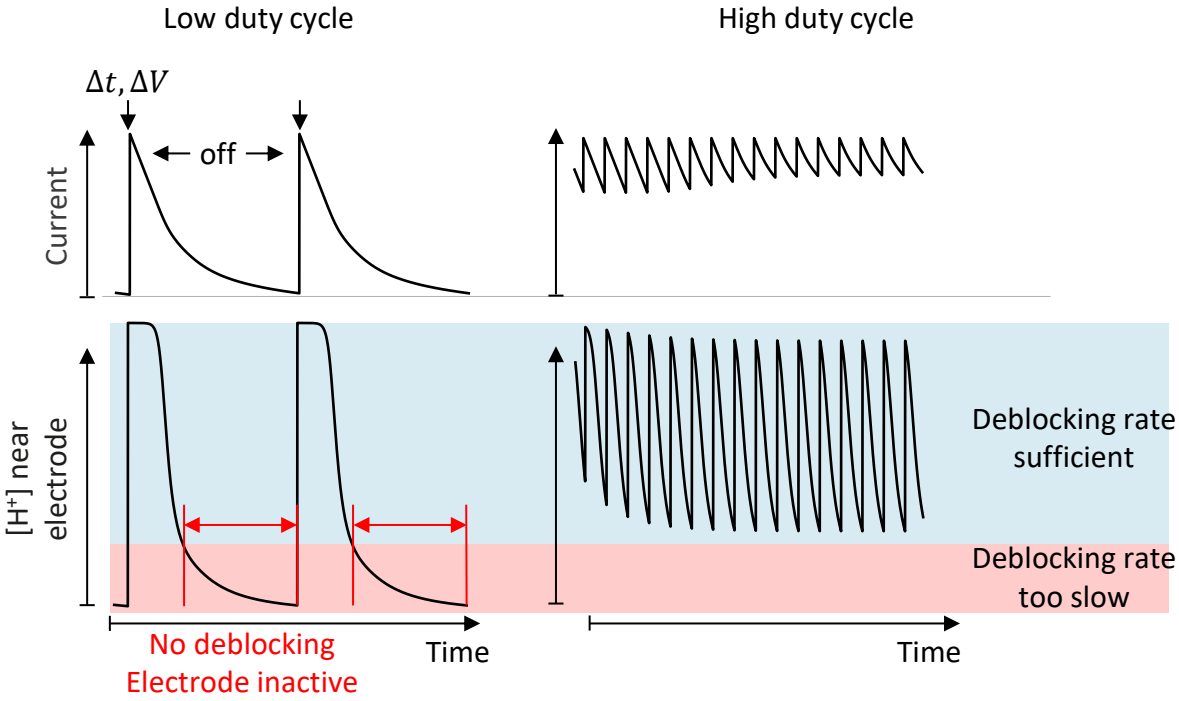

Our **experimental test device** consists of a micro-electrode array with 36 (6×6) externally driven platinum **ring-disk pairs**

Disks: Individually addressed working electrodes
Rings: common counter electrodes

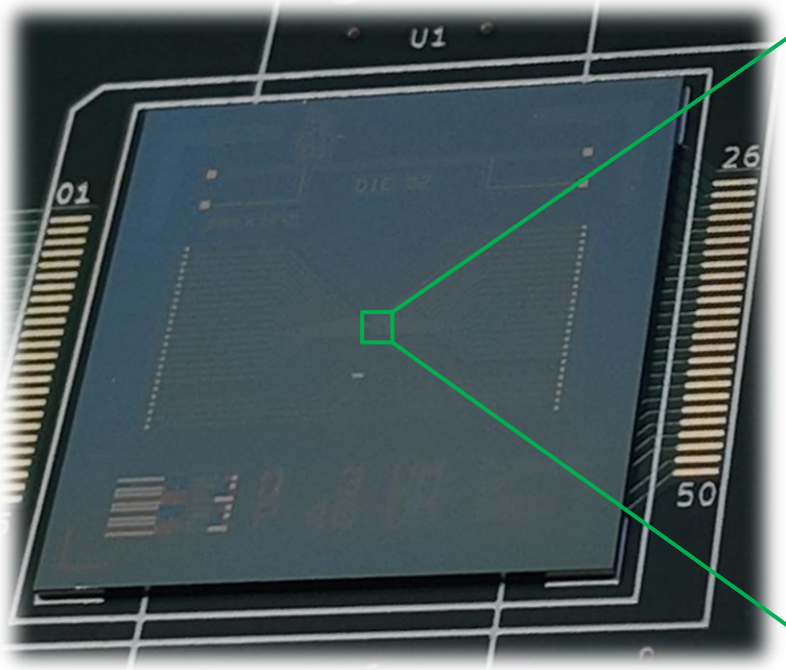

26 mm

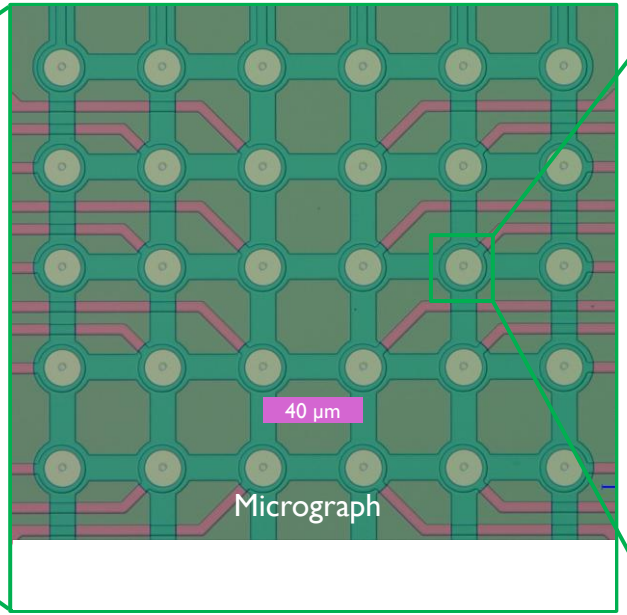

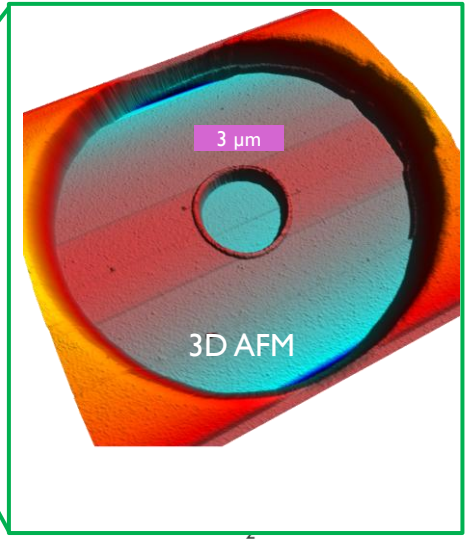

6x6 micro-electrode array
40 µm center-to-center pitch

d_1 = 3 µm h_1 = 200 nm
d_2 = 15 µm h_2 = 200 nm

imec

Experimentally, the **maximal off-time** is **1–5 ms** and largely determines the **efficiency** of **acid generation**

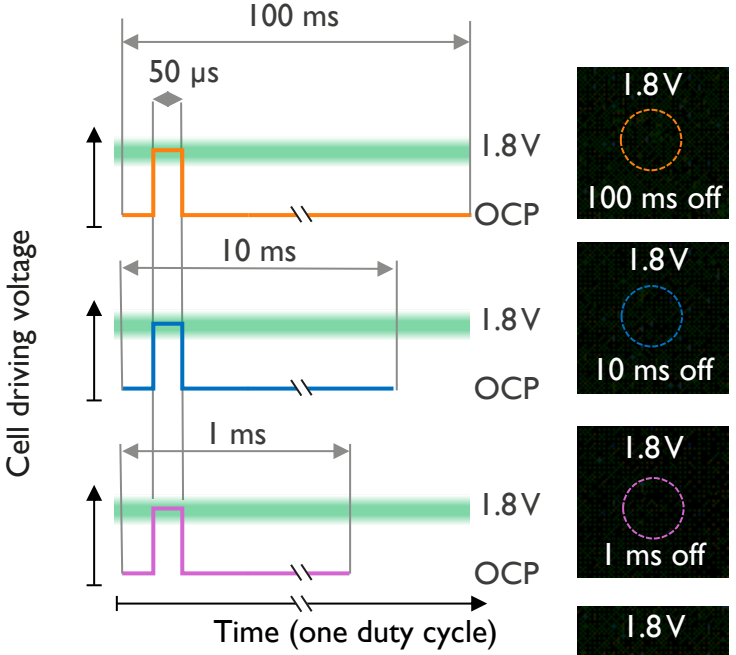

Electrolyte (90/10 ACN/MeOH):
50/10/10 mM HQ/BQ/Lut
50 mM TEAPS
10 nM pHrodo green

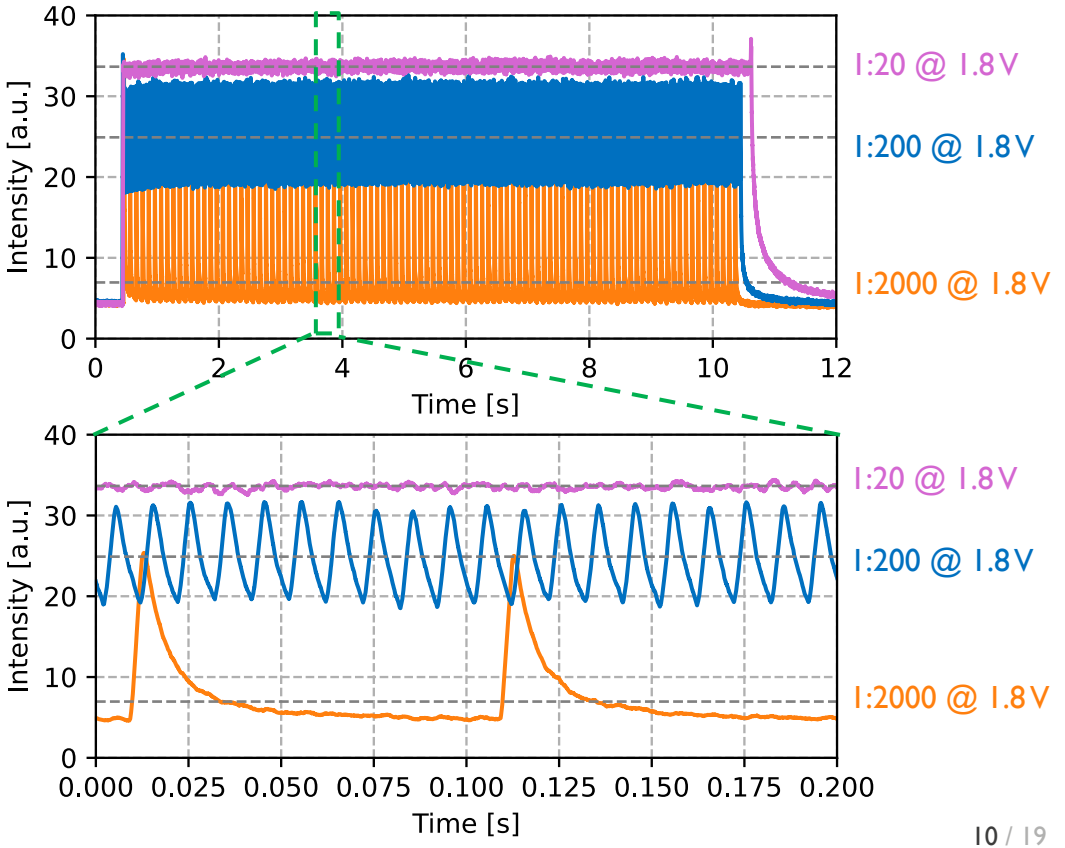

Modestly **increasing the driving voltage** from 1.8 to 2.5 V allows for **increasing the off-time** by an **order of magnitude**

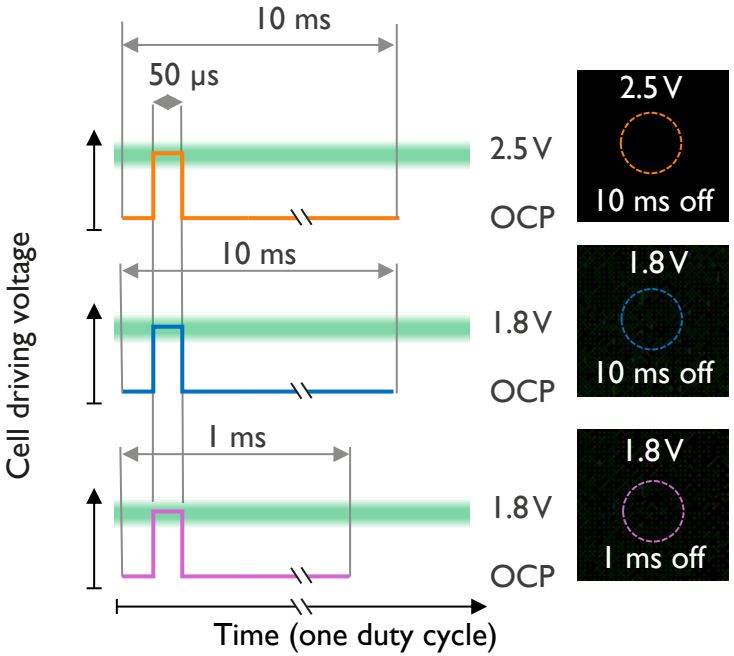

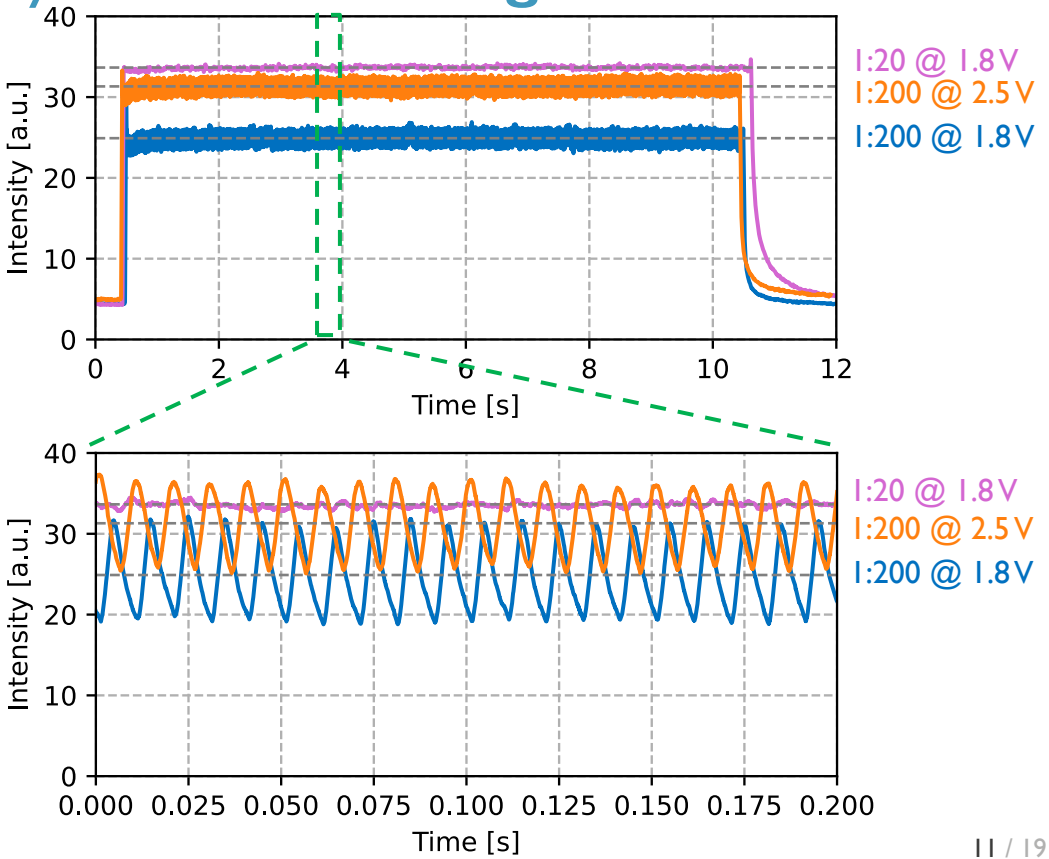

Electrolyte (90/10 ACN/MeOH):
50/10/10 mM HQ/BQ/Lut
50 mM TEAPS
10 nM pHrodo green

Multiple electrodes can be **activated simultaneously** by sequential **dynamic addressing** within a **single duty cycle**

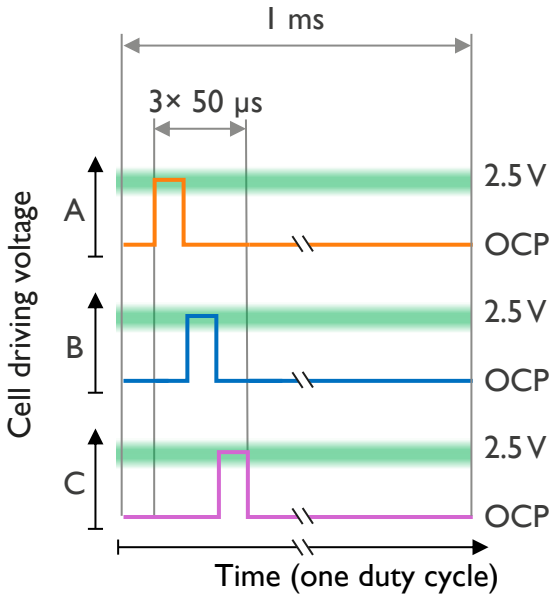

Addressing conditions:
50 µs on @ 2.5 V
1 ms off @ OCP

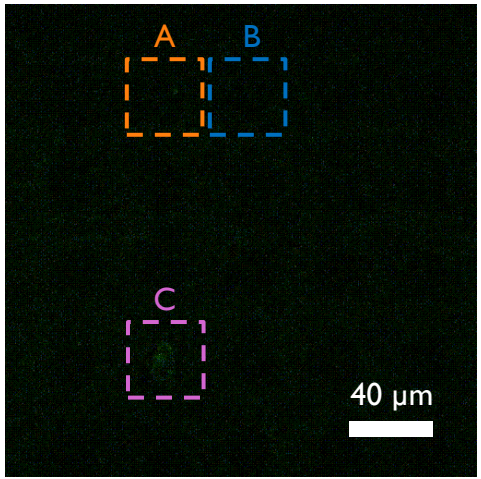

Electrolyte (90/10 ACN/MeOH):
50/10/10 mM HQ/BQ/Lut
50 mM TEAPS
10 nM pHrodo green

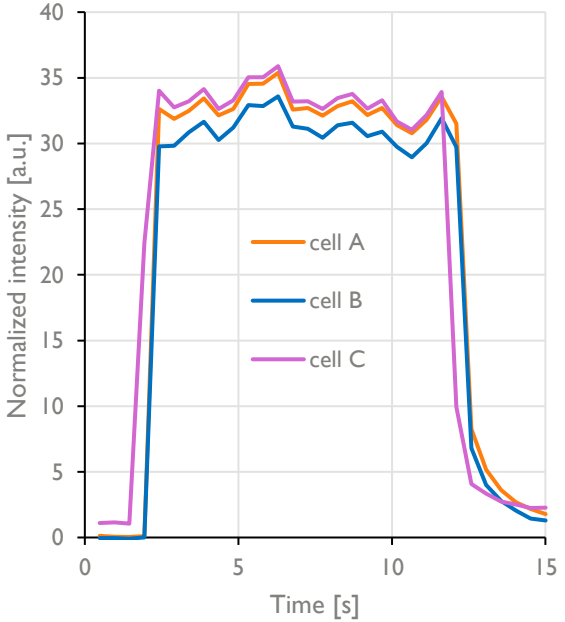

Our setup consists of a combination of **commercial** and **custom-build hardware**, controlled by **in-house developed software**

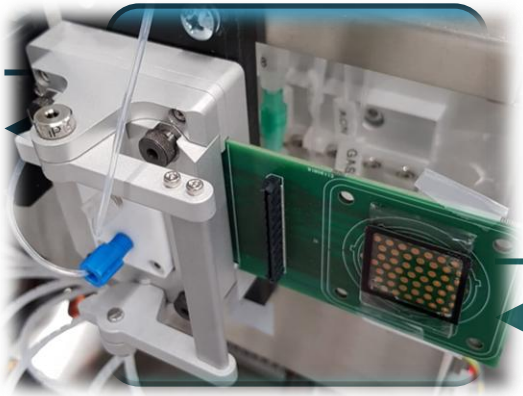

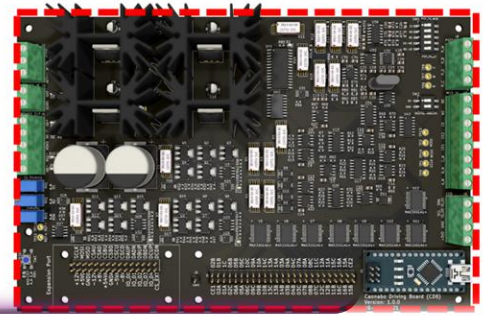

Dynamic and **static** addressing have a **comparable** electrochemical **deblocking strength**

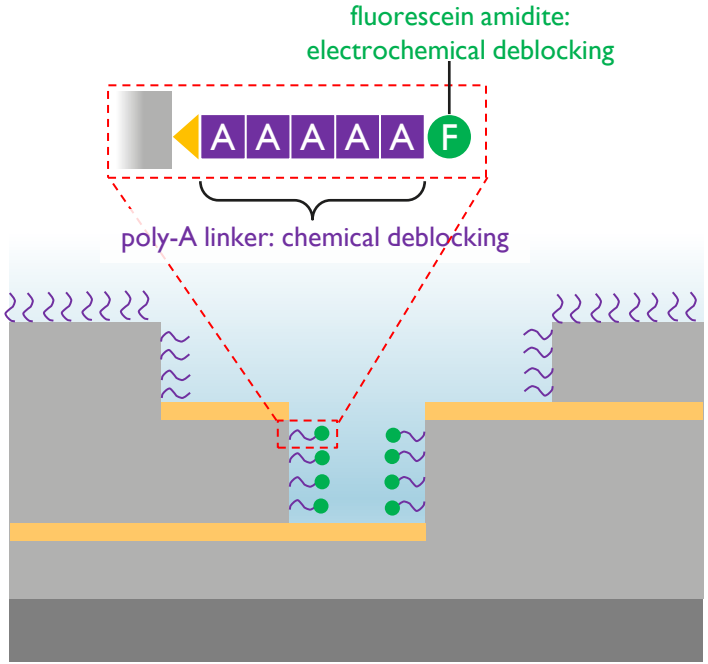

Electrolyte (90/10 ACN/MeOH):
50/10/10 mM HQ/BQ/Lut
50 mM TEAPS

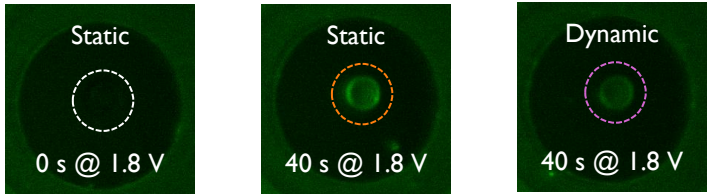

On: 50 µs
Off: 5 ms

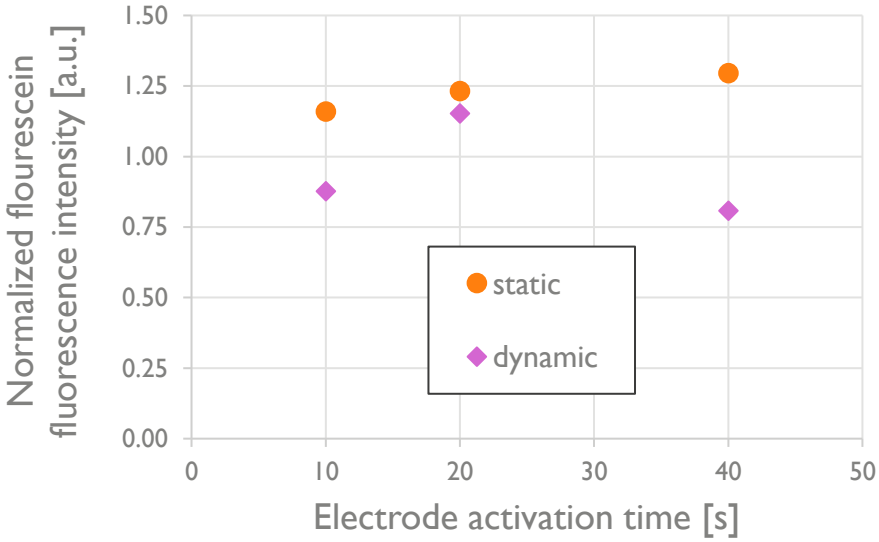

A **compact model** including **electrical** and **electrochemical** circuits enables **semi-quantitative non-steady-state** analysis

Full circuit for a single synthesis site

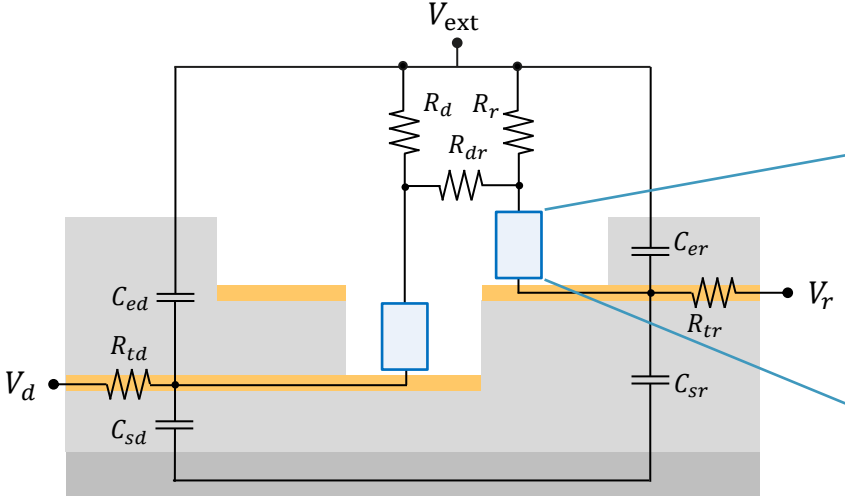

Implementation of an electrode interface

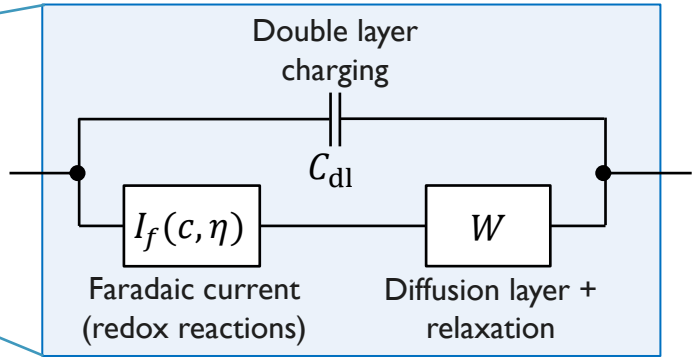

- Electrochemical cell
  → Model ring-disk electrode pair and electrolyte
- Device tracks
  → Include impact of parasitic impedance

- Faradaic current
  → Reaction kinetics quinone/hydroquinone
- Diffusion layer + relaxation
  → Mass transfer of active species

imec

In our test device, the **electrochemical current** is mainly sustained by **parasitic capacitance** of the **tracks**

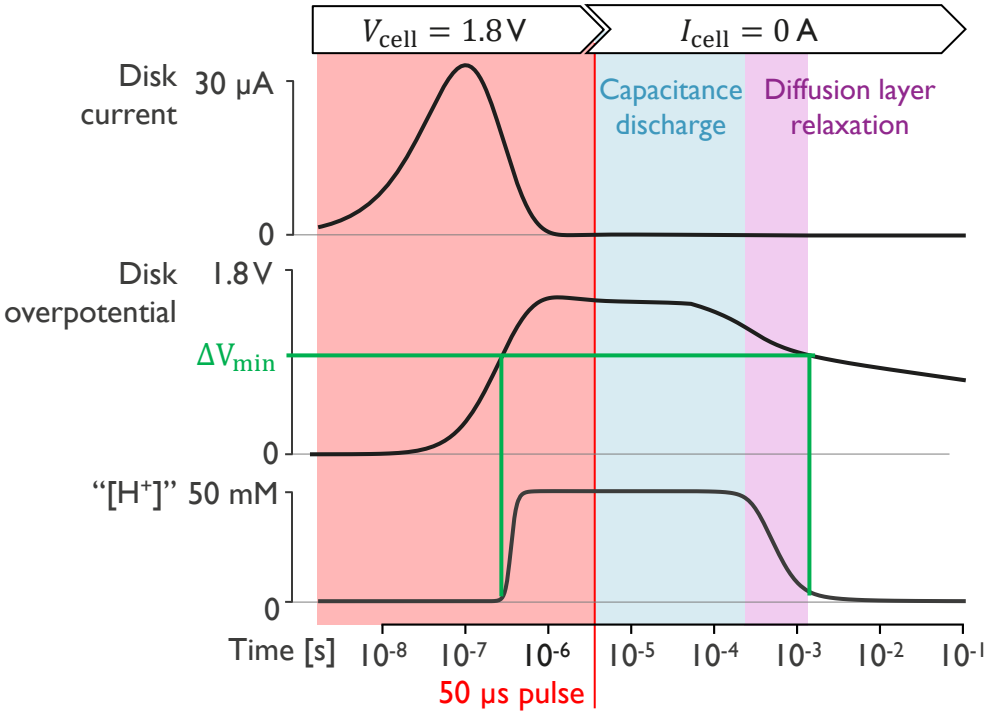

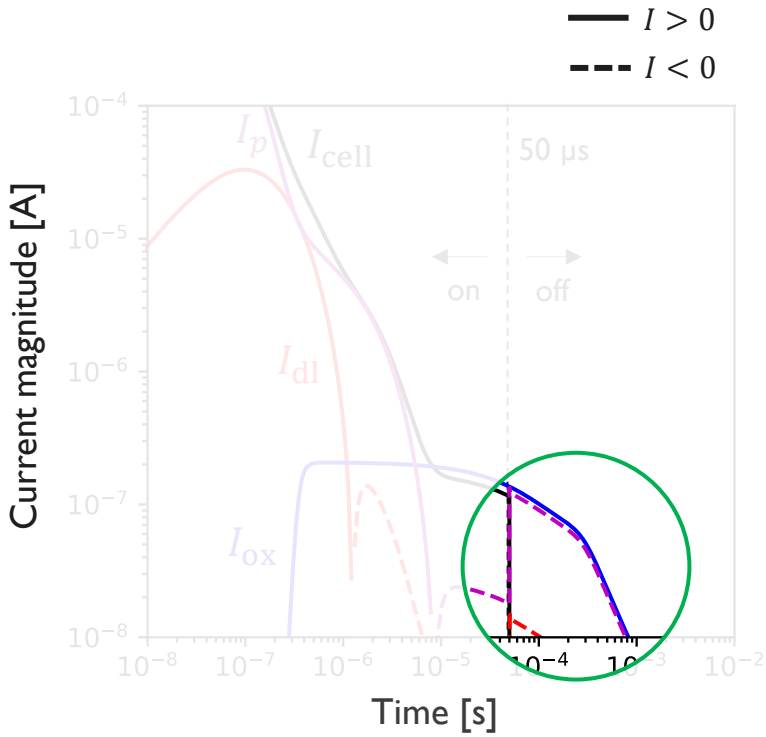

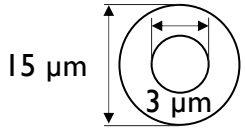

Track length ≈5 mm
Avg. track width ≈50 µm

imec

If the **EDL capacitance** and **electrolyte conductivity** are **high**, **scaled devices** (~100 nm pitch) can reach **1:1000** on:off ratios

Experimental test electrodes (WE: Ø3 µm)

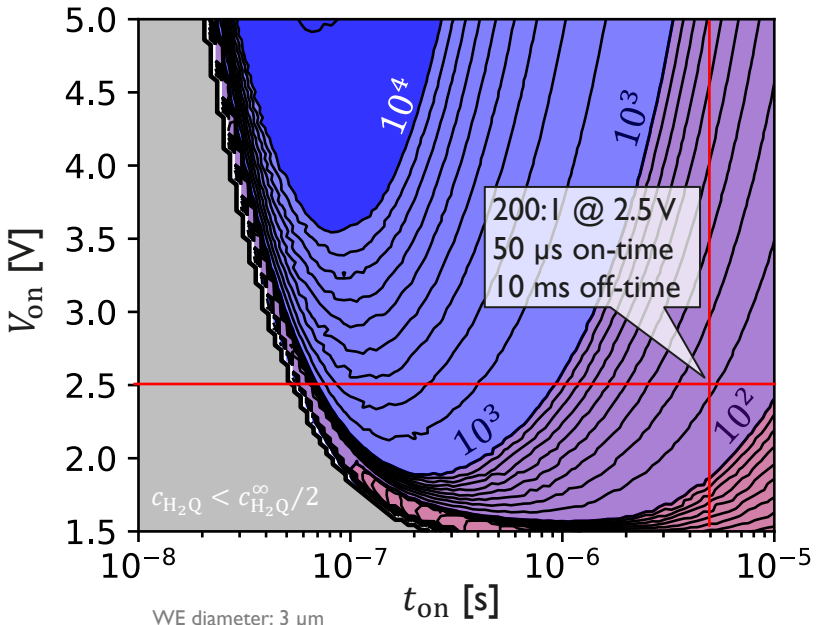

WE diameter: 3 µm
CE diameter: 15 µm
Track length: 5 mm
Avg. track width: 50 µm
Assumed double layer capacitance: ≈1 F/m²
Assumed electrolyte conductivity: ≈1.5 S/m

t_{off} when $c_{H_2Q} = c^{\infty}_{H_2Q}/2$

Scaled electrodes (WE: Ø30 nm)

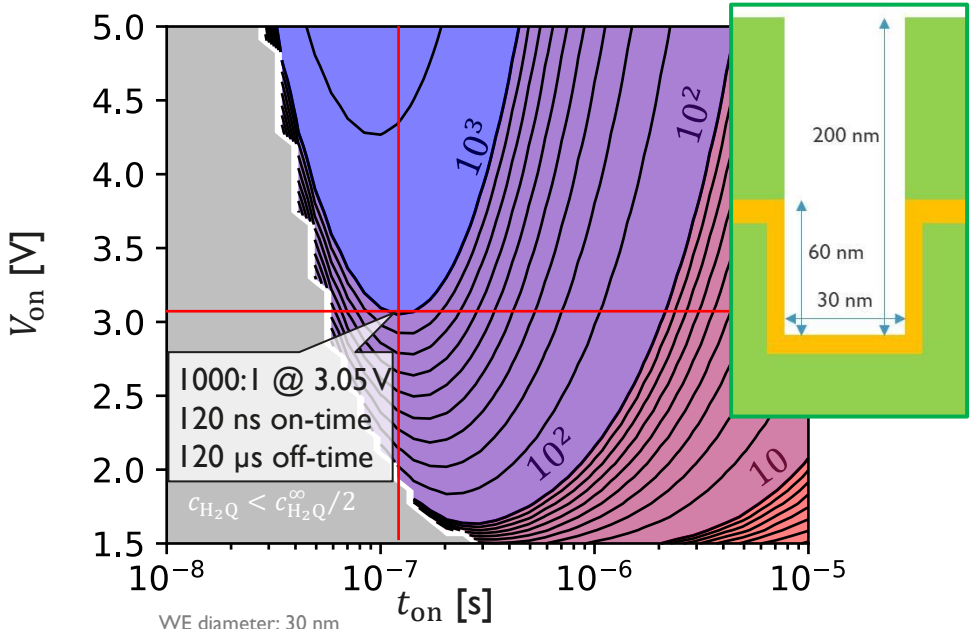

WE diameter: 30 nm
CE diameter: 80 nm
Track length & width: n.a.
Assumed double layer capacitance: ≈9 F/m²
Assumed electrolyte conductivity: ≈10 S/m

imec

Conclusions and outlook

- To **further scale** the electrochemical synthesis cell, one must **transition** from **static** ("SRAM"-like) to **dynamic** ("DRAM"-like) **addressing** architectures

- **Simulations** and **experiments** indicate that **dynamic addressing** can maintain a **consistently high proton** concentration for effective **deblocking**

- **Experimentally** observed **time-scales agree with simulations** for passive microelectrode array

- To develop the concept, **further electrode scaling** to **relevant device length-scales** and **CMOS integration** is needed

Acknowledgements

- The SC-DNA 2025 organizers
- My co-authors @ imec
  - Senne Fransen
  - Himanshu Sharma
  - Xiaoping Song
  - Sybren Santermans
  - Giedrius Degutis
  - Kathrin Hölz
  - Christina Avdikou
  - Olivier Y.F. Henry
  - Karolien Jans
  - César Javier Lockhart de la Rosa
  - Arnaud Furnémont
- Other contributors @ imec
  - Karolien Jans
  - Tim Stakenborg
  - Ahmed Taher
  - Naghmeh Fatemi
  - Farrukh Yasin
  - Jelle Fondu
  - Liesbet Lagae
  - Paru Deshpande
  - Rabea Hanifa
  - Wiebe Vanhove


imec
embracing a better life

Diffusion layer relaxation model

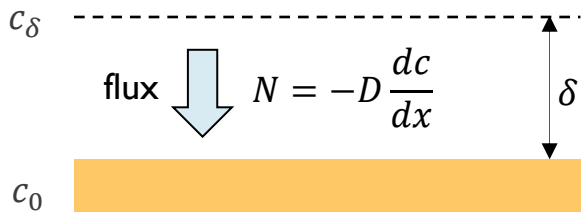

Finite thickness Warburg element
in **frequency domain**

$$\widehat{N}(\omega) = H(\omega)\Delta c(\omega)$$

Add correct equation

Finite thickness Warburg element
in **time domain**

$$N(t) = \frac{D}{\delta}(c_\delta - c_0) - \frac{2D}{\ell}\int_0^t \sum_{n=1}^{\infty} e^{-\frac{n^2\pi^2 D(t-\tau)}{\delta^2}} \frac{dc_0}{d\tau}\, d\tau$$

Practical **compact model**
(first order approximation)

$$\frac{3\delta}{\pi^2}\frac{dc_0}{dt} = -\frac{D}{\delta}(c_\delta - c_0) + \left(N(t) + \frac{\delta^2}{\pi^2 D}\frac{dN}{dt}\right)$$

The flux N follows from the kinetics
of the electrochemical reactions

imec

Faradaic reactions

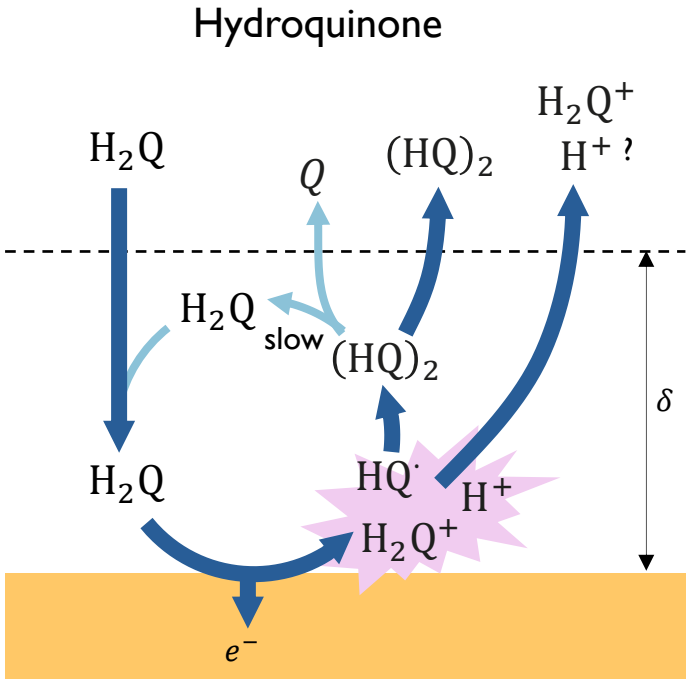

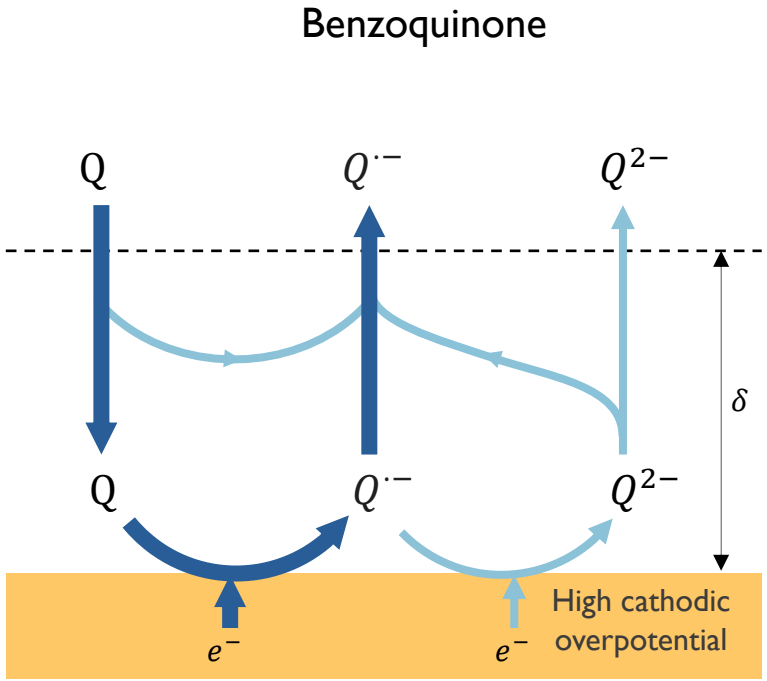

Parameter estimation through literature & independent experiments

Components
Hydroquinone
Benzoquinone
50 mM TBAPF

Dissolved in
10 vol% MeOH
90 vol% Acetonitrile

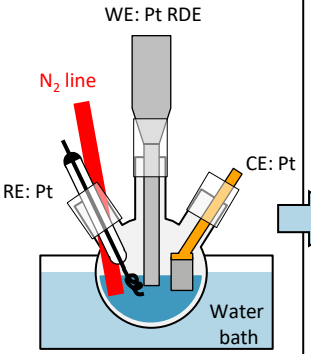

$$\frac{\partial c_{H_2Q}}{\partial t} = D_{H_2Q}\frac{\partial^2 c_{H_2Q}}{\partial x^2} - \frac{a\Omega^{3/2}x^2}{\nu^{1/2}}\frac{\partial c_{H_2Q}}{\partial x} + R_2 \qquad -D_{H_2Q}\frac{\partial c_{H_2Q}}{\partial x}\Big|_0 = -S_1$$

$$\frac{\partial c_{H_2Q^{+\cdot}}}{\partial t} = D_{H_2Q^{+\cdot}}\frac{\partial^2 c_{H_2Q^{+\cdot}}}{\partial x^2} - \frac{a\Omega^{3/2}x^2}{\nu^{1/2}}\frac{\partial c_{H_2Q^{+\cdot}}}{\partial x} - 2R_1 \qquad -D_{H_2Q^{+\cdot}}\frac{\partial c_{H_2Q^{+\cdot}}}{\partial x}\Big|_0 = S_1$$

$$\frac{\partial c_Q}{\partial t} = D_Q\frac{\partial^2 c_Q}{\partial x^2} - \frac{a\Omega^{3/2}x^2}{\nu^{1/2}}\frac{\partial c_Q}{\partial x} + R_2 \qquad -D_Q\frac{\partial c_Q}{\partial x}\Big|_0 = -S_2 - S_3$$

$$\frac{\partial c_{H^+}}{\partial t} = D_{H^+}\frac{\partial^2 c_{H^+}}{\partial x^2} - \frac{a\Omega^{3/2}x^2}{\nu^{1/2}}\frac{\partial c_{H^+}}{\partial x} + 2R_1 \qquad -D_{H^+}\frac{\partial c_{H^+}}{\partial x}\Big|_0 = -S_2$$

$$\frac{\partial c_{(HQ)_2}}{\partial t} = D_{(HQ)_2}\frac{\partial^2 c_{(HQ)_2}}{\partial x^2} - \frac{a\Omega^{3/2}x^2}{\nu^{1/2}}\frac{\partial c_{(HQ)_2}}{\partial x} + R_1 - R_2 \qquad -D_{(HQ)_2}\frac{\partial c_{(HQ)_2}}{\partial x}\Big|_0 = \frac{S_2}{2}$$

$$\frac{\partial c_{Q^{-\cdot}}}{\partial t} = D_{Q^{-\cdot}}\frac{\partial^2 c_{Q^{-\cdot}}}{\partial x^2} - \frac{a\Omega^{3/2}x^2}{\nu^{1/2}}\frac{\partial c_{Q^{-\cdot}}}{\partial x} \qquad -D_{Q^{-\cdot}}\frac{\partial c_{Q^{-\cdot}}}{\partial x}\Big|_0 = S_3$$

$$H_2Q \rightarrow H_2Q^{+\cdot} + e^- \qquad S_1 = k_{ox}c_{H_2Q}\exp\left(\frac{\alpha_1 F\eta}{RT}\right)$$

$$Q + H^+ + e^- \rightarrow (HQ)_2/2 \qquad S_2 = k_{red}c_Q c_H \exp\left(-\frac{\alpha_2 F\eta}{RT}\right)$$

$$Q + e^- \rightleftharpoons Q^{-\cdot} \qquad S_3 = k_0\left\{c_Q\exp\left(-\frac{\alpha_3 F[\eta - E_0]}{RT}\right) - c_{Q^{-\cdot}}\exp\left(\frac{\alpha_3 F[\eta - E_0]}{RT}\right)\right\}$$

$$2H_2Q^{+\cdot} \rightarrow (HQ)_2 + 2H^+ \qquad R_1 = k_1 c_{H_2Q^{+\cdot}}^2$$

$$(HQ)_2 \rightarrow Q + H_2Q \qquad R_2 = k_2 c_{(HQ)_2}$$

Parameters

$D_{H_2Q} = 2.8 \times 10^{-9}\ m^2/s$
$D_{H_2Q^{+\cdot}} = D_{H_2Q}$
$D_Q = 3.2 \times 10^{-9}\ m^2/s$
$D_{Q^{-\cdot}} = D_Q$
$D_{H^+} =$
$D_{(HQ)_2} = 1 \times 10^{-9} - 2 \times 10^{-9}\ m^2/s$

$k_{ox} = 8 \times 10^{-13}\ m/s$
$k_{red} = 4 \times 10^{-3}\ m/s$
$k_1 > 1500\ m^3/mol.\,s$
$k_2 > 1000\ s^{-1}$
$E_0 = -0.45\ V$
$\alpha_1 = \alpha_2 = \alpha_3 = 0.5$

Proton Effects in the Electrochemistry of the Quinone Hydroquinone System in Aprotic Solvents
B. R. Eggins and J. Q. Chambers†
Department of Chemistry, University of Colorado, Boulder, Colorado
J. Electrochem. Soc. (1970)

Acid/base and hydrogen bonding effects on the proton-coupled electron transfer of quinones and hydroquinones in acetonitrile: Mechanistic investigation by voltammetry, ^{1}H NMR and computation
Timothy M. Alligrant[a], John C. Hackett[b], Julio C. Alvarez[a,*]
E. Acta (2010)

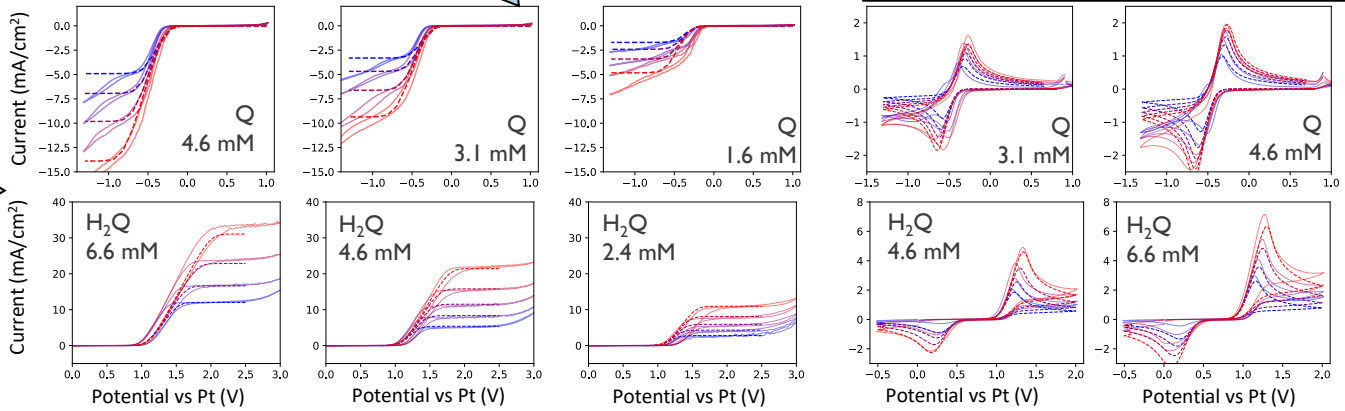

Simplified model for microelectrode simulation

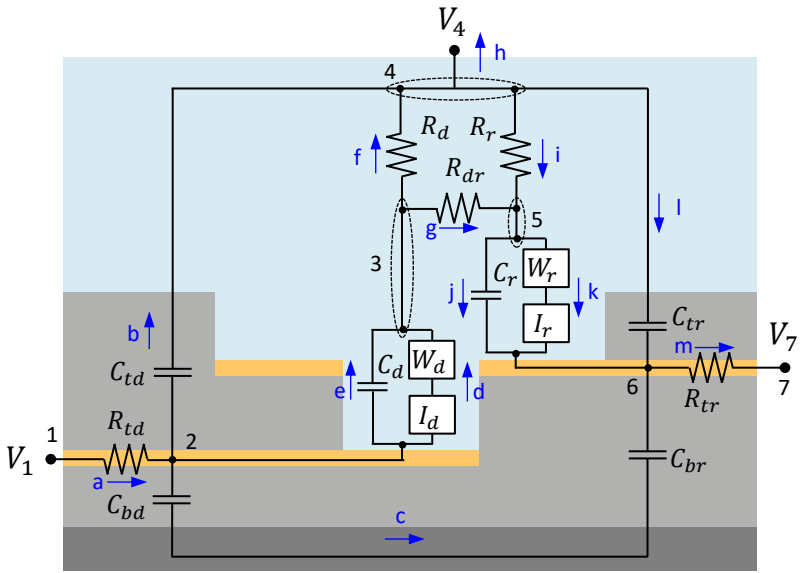

Node 2	$0 = I_a - I_b - I_c - I_d - I_e$
Node 3	$0 = I_d + I_e - I_f - I_g$
Node 4	$0 = I_b + I_f - I_i - I_l$
Node 5	$0 = I_g + I_i - I_j - I_k$
Node 6	$0 = I_j - I_k + I_l + I_c - I_m$
Track R	$0 = V_1 - V_2 - R_{td} I_a$
Track C	$0 = C_{td}\left(\dot{V}_2 - \dot{V}_4\right) - I_b$
Track C	$0 = \left(C_{bd}^{-1} + C_{br}^{-1}\right)^{-1}\left(\dot{V}_2 - \dot{V}_6\right) - I_c$
HQ ox	$0 = I_d - A_d F k_d c_{\mathrm{H_2Q}} \exp\left(\frac{\alpha_{\mathrm{ox}} F}{RT}(V_2 - V_3)\right)$
Disk C	$0 = C_d\left(\dot{V}_2 - \dot{V}_3\right) - I_e$
Warburg	$0 = \frac{3\ell_d}{\pi^2}\dot{c}_{\mathrm{H_2Q}} - \frac{D_{\mathrm{H_2Q}}}{\ell_d}\left(c_{\mathrm{H_2Q}}^{\infty} - c_{\mathrm{H_2Q}}\right) + \frac{1}{n_e F A_d}\left(I_d + \frac{\ell_d^2}{\pi^2 D_{\mathrm{H_2Q}}}\dot{I}_d\right)$
Disk R	$0 = V_3 - V_4 - R_d I_f$
Liquid R	$0 = V_3 - V_5 - R_{dr} I_f$
Q red	$0 = I_k - A_r k_r F \begin{bmatrix} c_{\mathrm{Q}} \exp\left(\frac{\alpha_{\mathrm{red}} F}{RT}(V_5 - V_6 + E_0)\right) \\ -\left(c_{\mathrm{Q}}^{\infty} - c_{\mathrm{Q}}\right)\exp\left(-\frac{(1-\alpha_{\mathrm{red}})F}{RT}(V_5 - V_6 + E_0)\right) \end{bmatrix}$
Ring C	$0 = C_r\left(\dot{V}_5 - \dot{V}_6\right) - I_j$
Warburg	$0 = \frac{3\ell_r}{\pi^2}\dot{c}_{\mathrm{Q}} - \frac{D_{\mathrm{Q}}}{\ell_r}\left(c_{\mathrm{Q}}^{\infty} - c_{\mathrm{Q}}\right) + \frac{1}{n_e F A_r}\left(I_r + \frac{\ell_r^2}{\pi^2 D_{\mathrm{Q}}}\dot{I}_r\right)$
Ring R	$0 = (V_4 - V_5) - R_r I_i$
Track C	$0 = C_{tr}\left(\dot{V}_4 - \dot{V}_6\right) - I_l$
Track R	$0 = V_6 - V_7 - R_{tr} I_m$

Typical response for experimental device

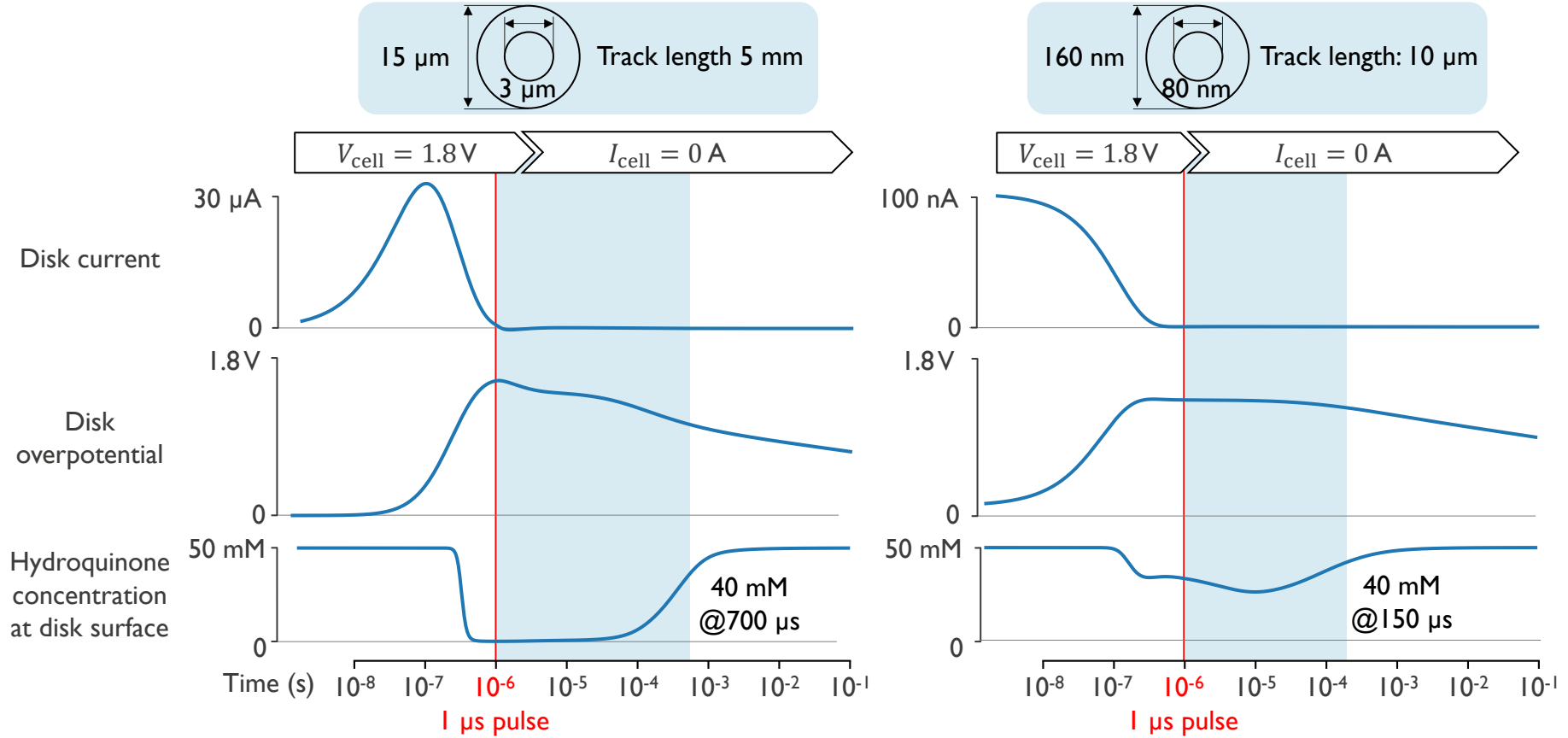

Geometry and corresponding compact circuit model

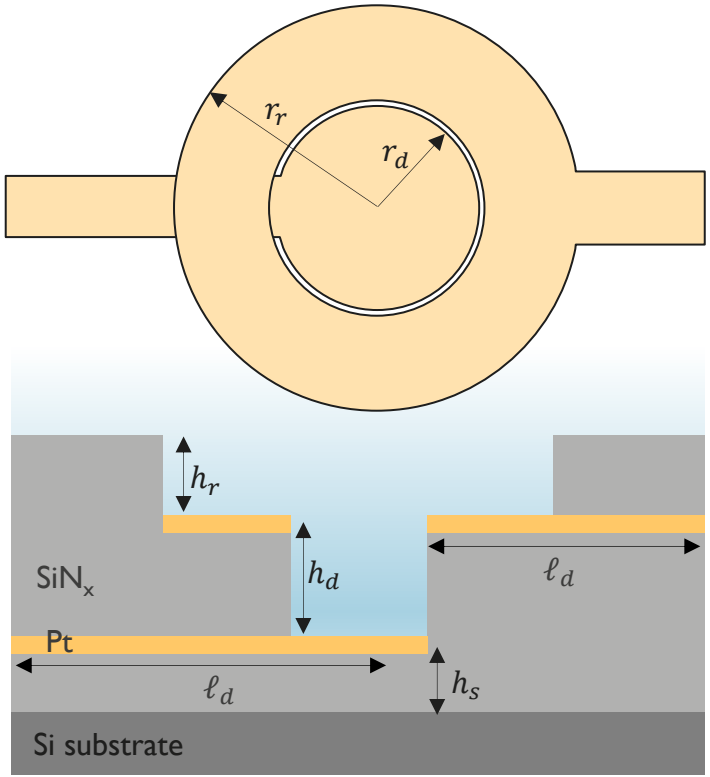

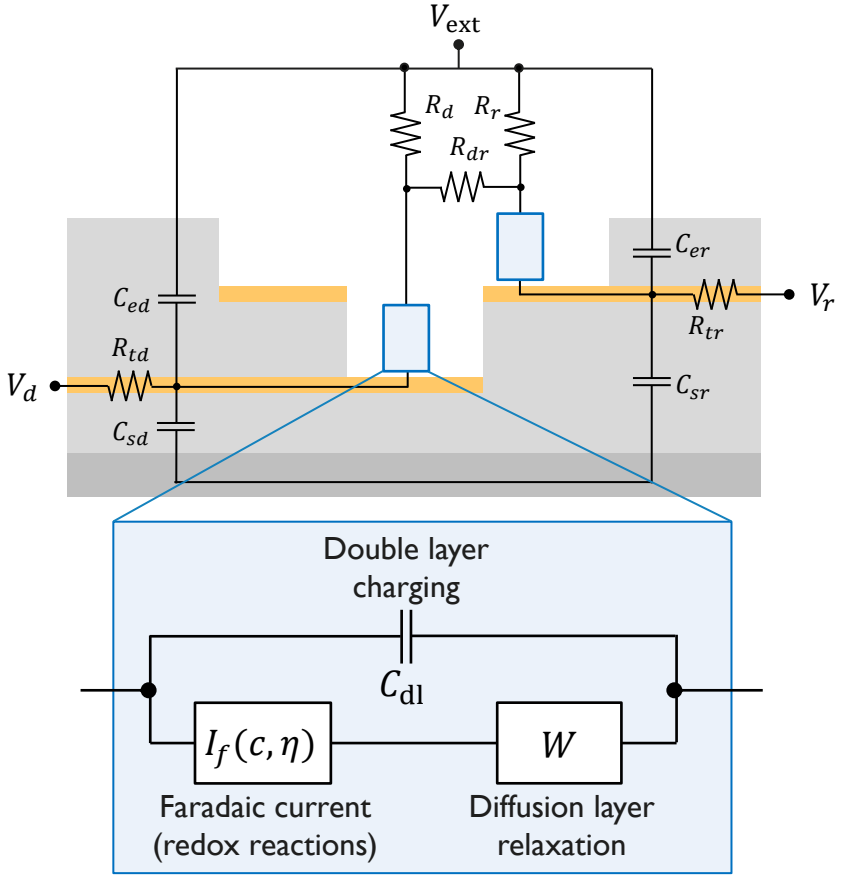

Harnessing DRAM concepts for high-density multiplexed electrode array addressing

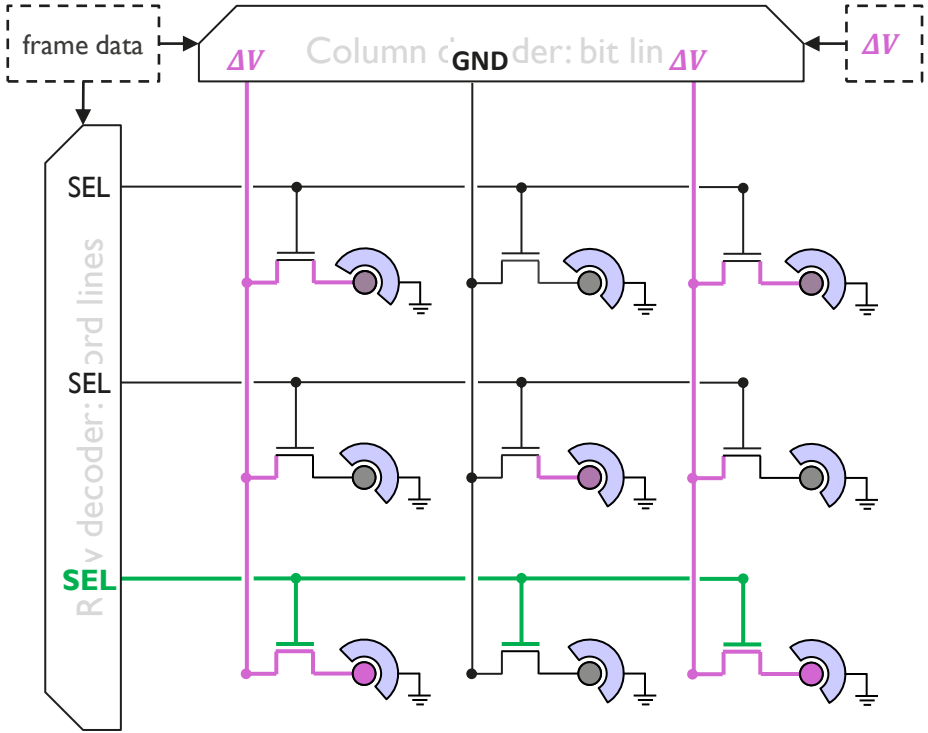

- Electrode activation pattern (“frame”) is loaded in separate memory array and send to synthesis array row-by-row
  - Row decoder sequentially activates each wordline, which turn on the access transistors
  - Synchronously, the column decoder sets the bitlines to either the driving voltage (“ON”) or ground (“OFF”)
  - Transient activation results in the charging of the cell capacitance
  - the resulting voltage difference then drives the electrochemical reaction, whose potential
- The transient charging of the capacitance of the cell allows for an electrochemical current
- This pattern is repeated until the electrochemical

Device topography (AFM) and x-section (FIB-SEM) characterization

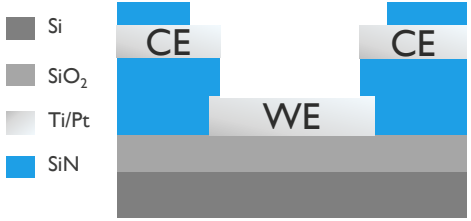

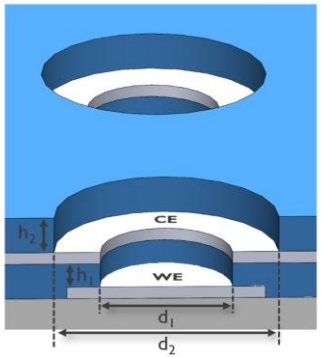

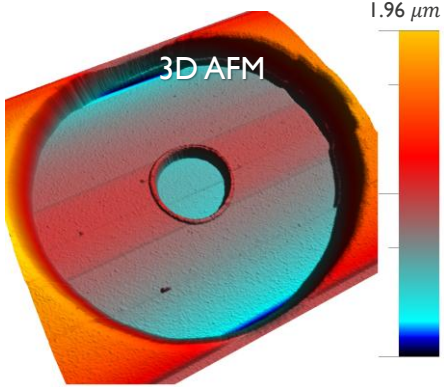

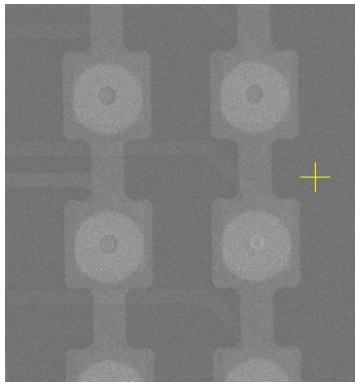

FIB-SEM

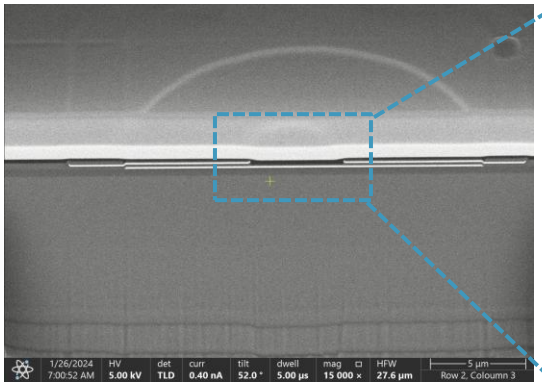

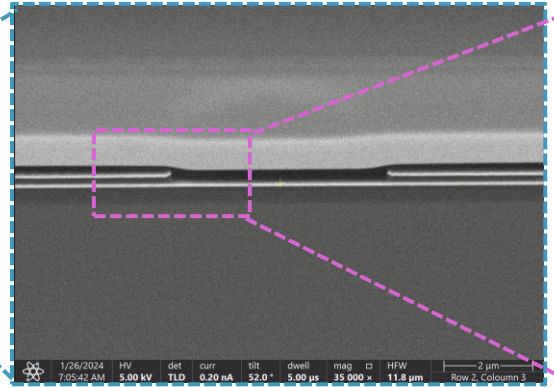

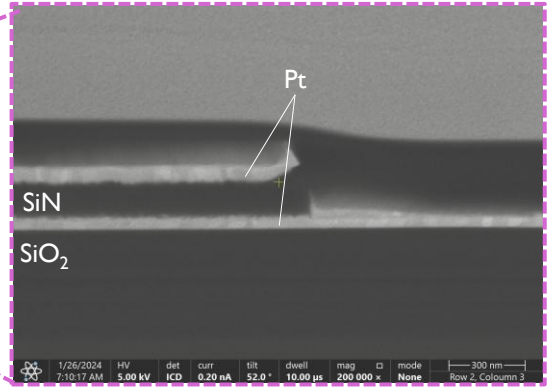

imec

Setup allows for simultaneous electrical and optical measurements

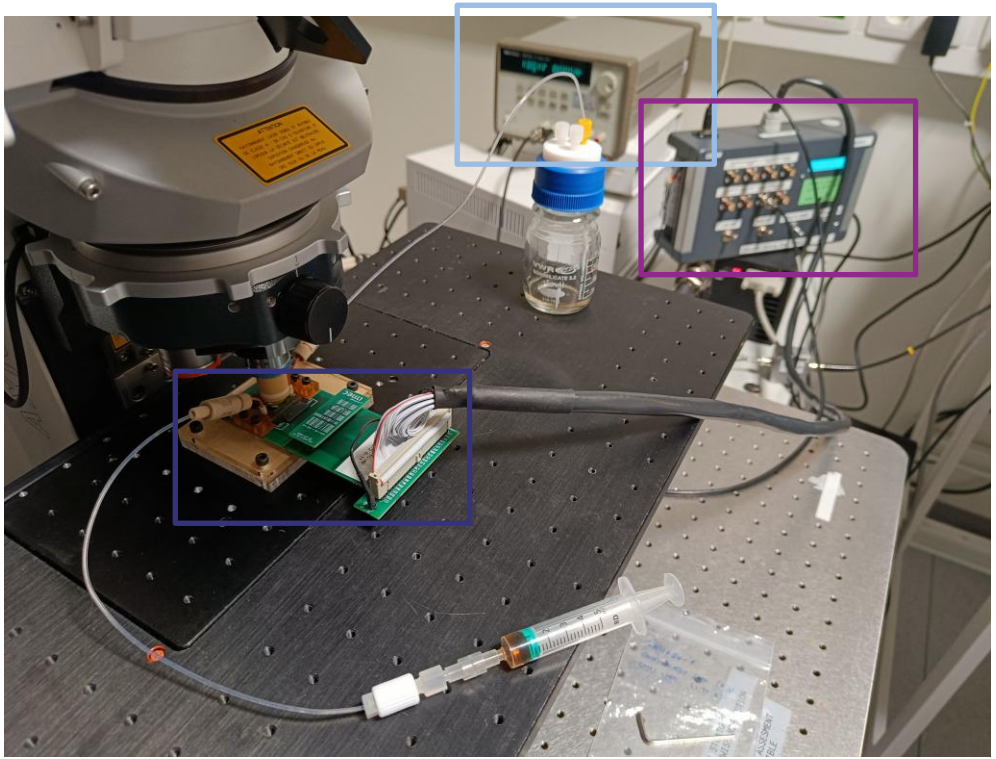

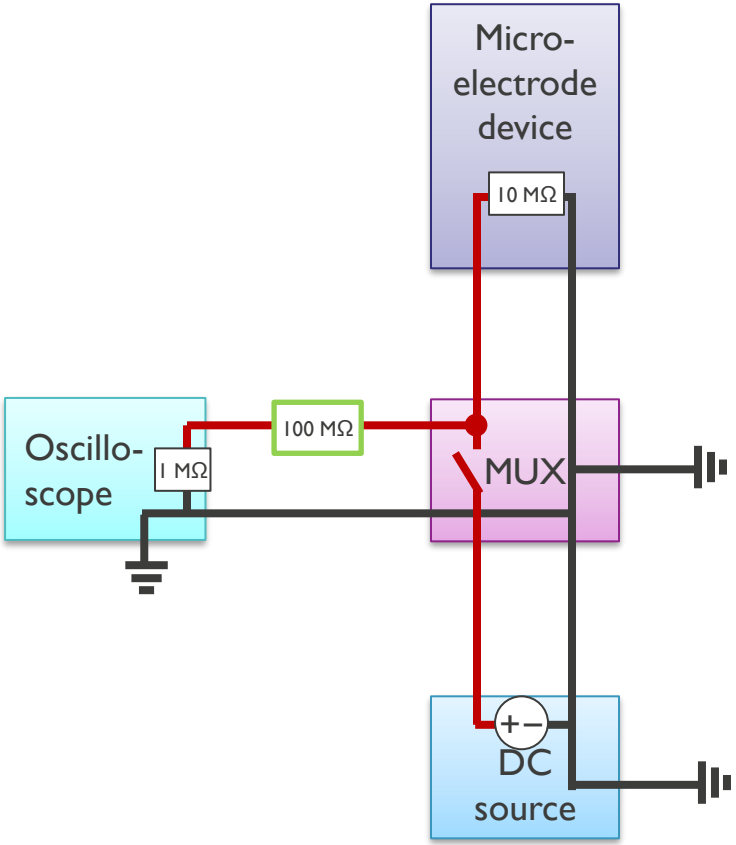

Impact of "off time" on the cell voltage

HQ/BQ 50/10 mM
10 mM lut
50 mM TEAPS
90:10 v/v% ACN/MeOH

50 µs on @ 2.5 V + 100 ms off @ OCP
(1/2000)

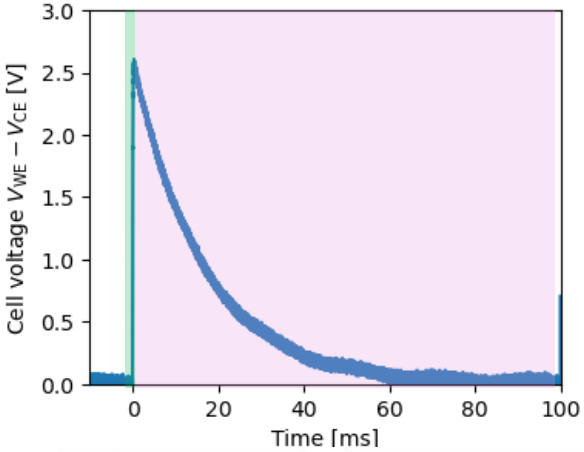

50 µs on @ 2.5 V + 10 ms off @ OCP
(1/200)

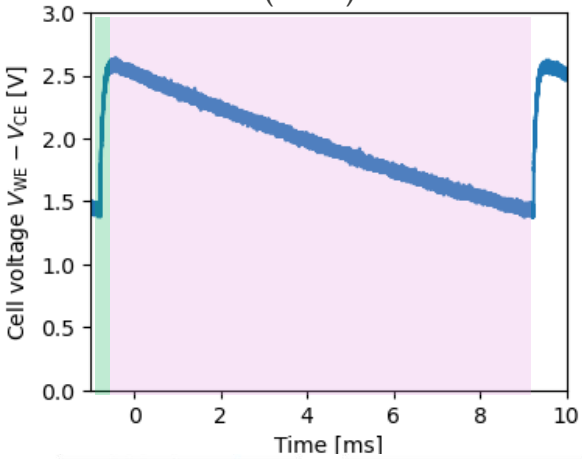

50 µs on @ 2.5 V + 1 ms off @ OCP
(1/20)

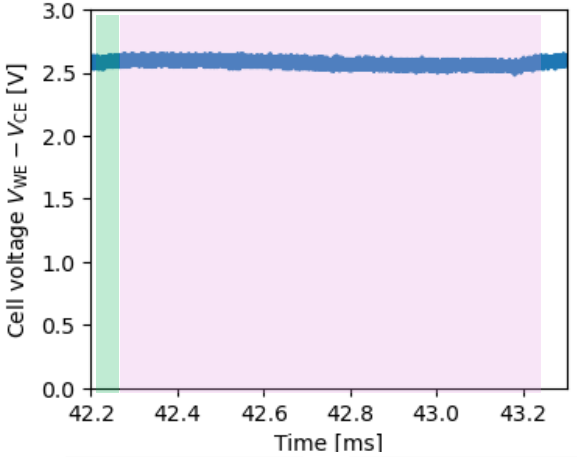

Fluorescence [a.u.]

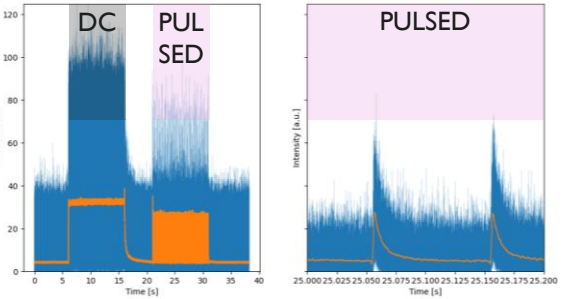

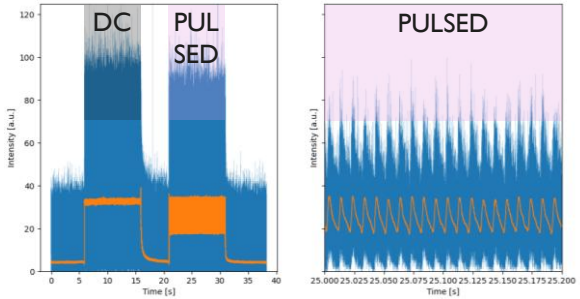

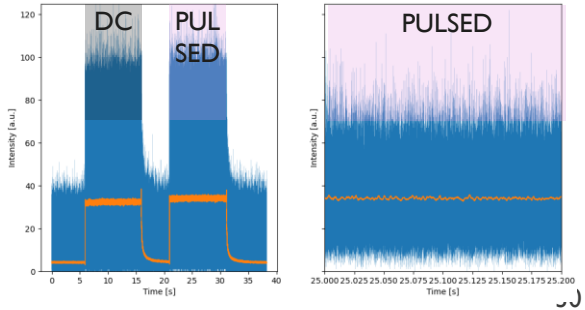

Impact of oscilloscope connection on the fluorescence intensity

10s on @ 1.8 V DC

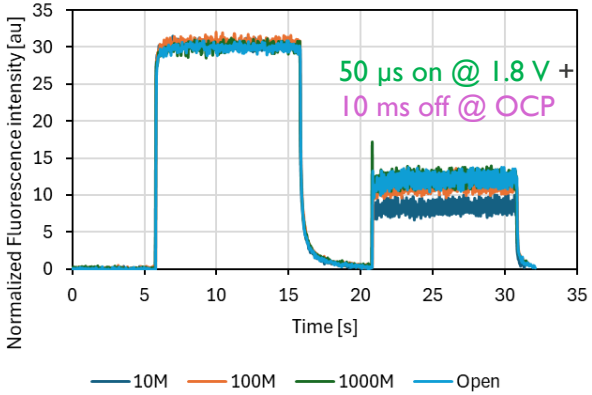

Low → high input resistance

10s on @ 1.8 V DC

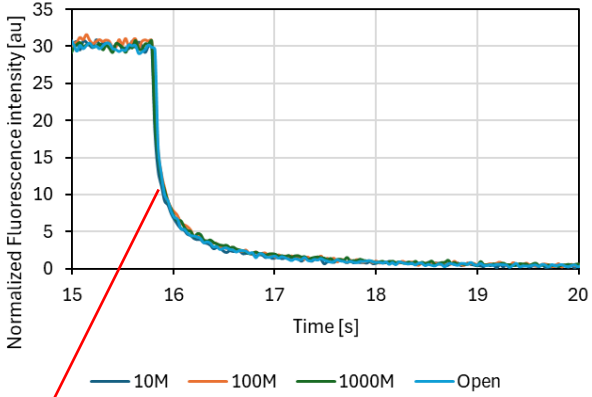

50 µs on @ 1.8 V + 10 ms off @ OCP (1/200)

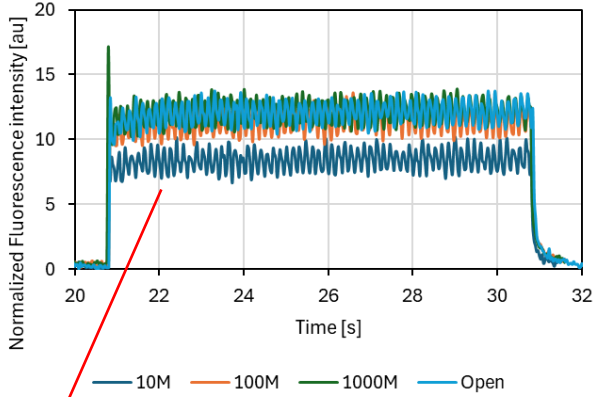

HQ/BQ 50/10 mM
10 mM lutidine
50 mM TEAPS
90:10 v/v% ACN/MeOH

No clear impact of oscilloscope connection and input resistance on decay in fluorescence intensity

During pulsing: Steady-state fluorescence intensity reduced when using low input resistance

20240613_pulsing_V1.8_0103MOhm_on000050_off100000_spot.czi

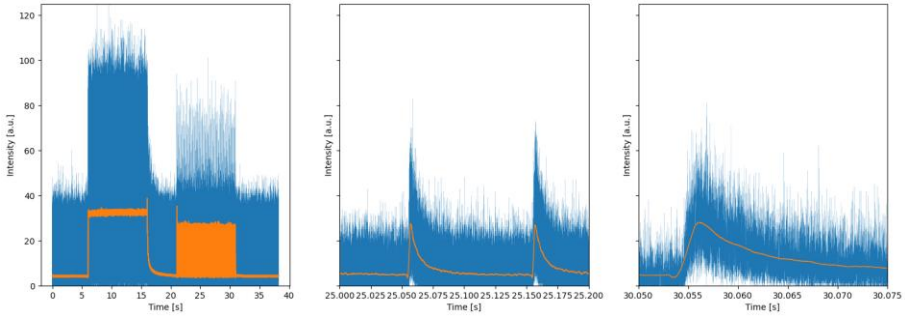

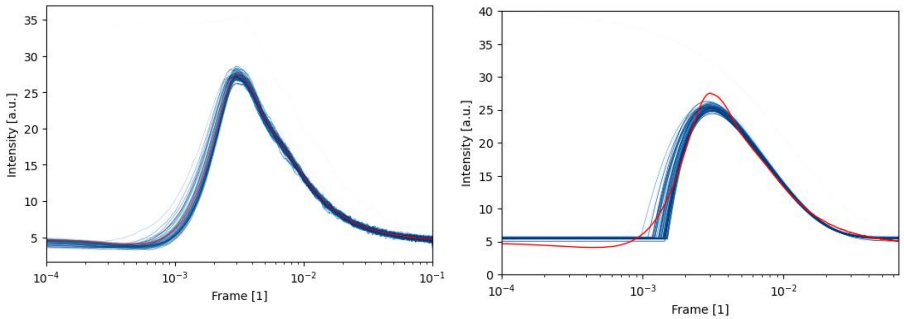

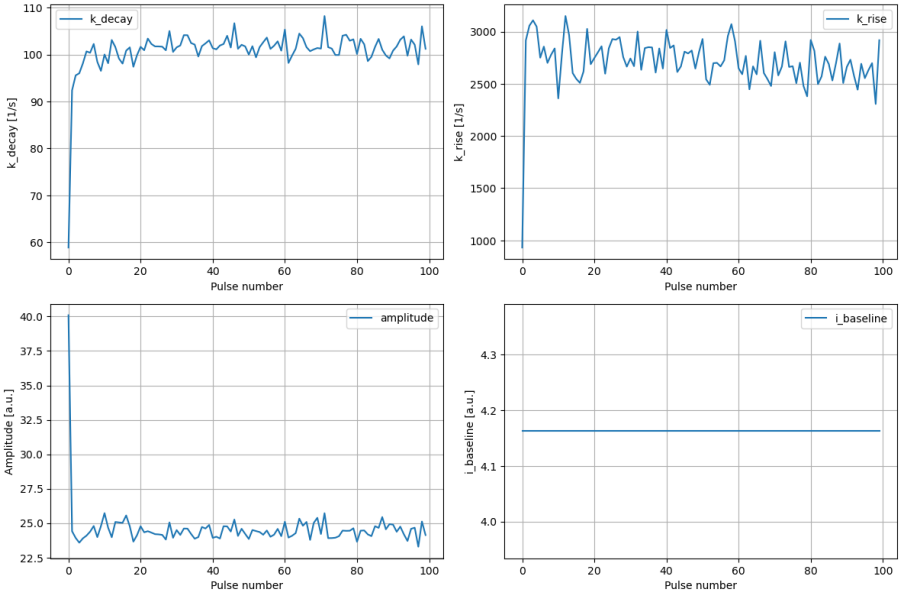

Mean k_decay: 100.93 1/s
Mean k_rise: 2712.23 1/s
Mean amplitude: 24.58 a.u.
Mean i_baseline: 4.16 a.u.

20240613_pulsing_V1.8_0103MOhm_on000050_off010000_spot.czi

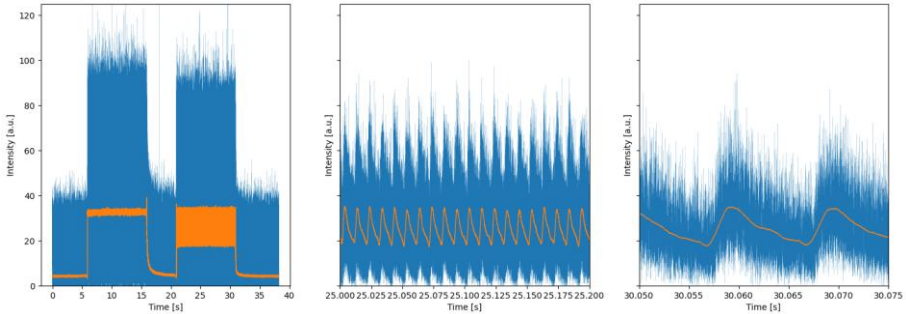

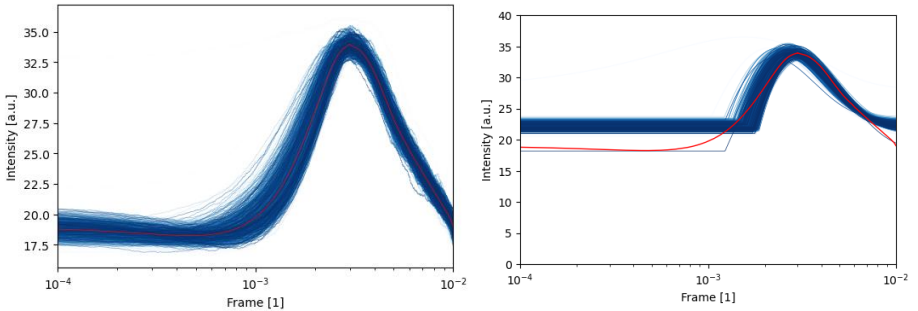

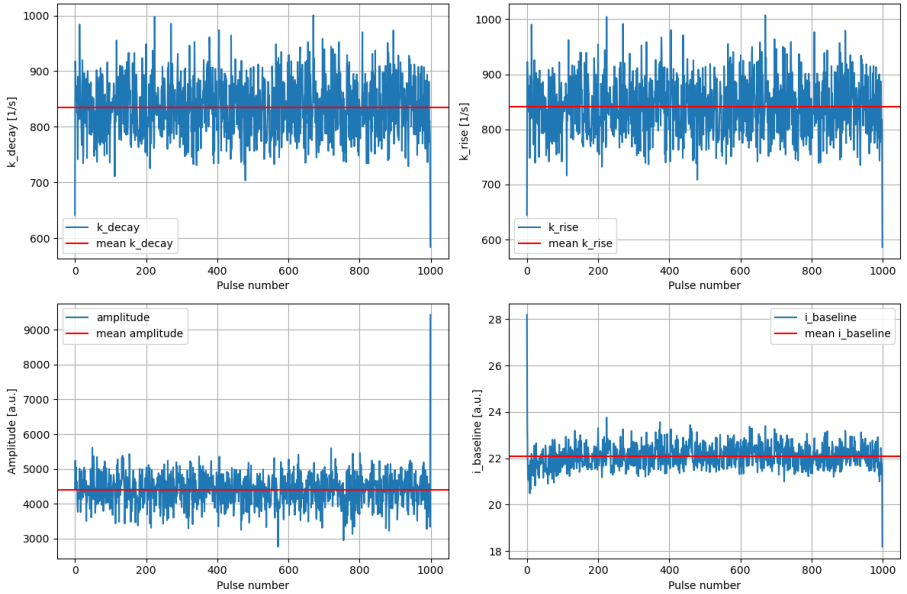

Mean k_decay: 835.04 1/s
Mean k_rise: 841.25 1/s
Mean amplitude: 4396.34 a.u.
Mean i_baseline: 22.09 a.u.

20240613_pulsing_V1.8_0103MOhm_on000050_off001000_spot.czi

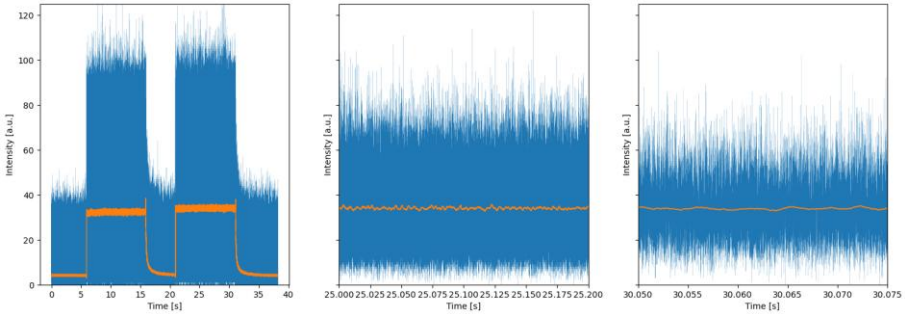

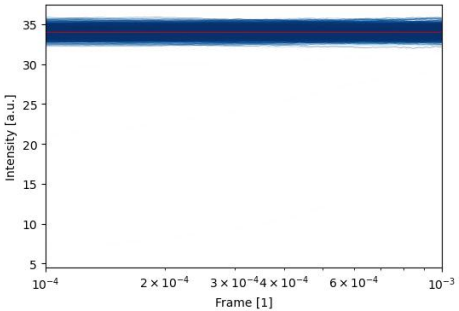

Mean baseline: 34.01 a.u.

20240613_pulsing_V2.5_0103MOhm_on000050_off010000_spot.czi

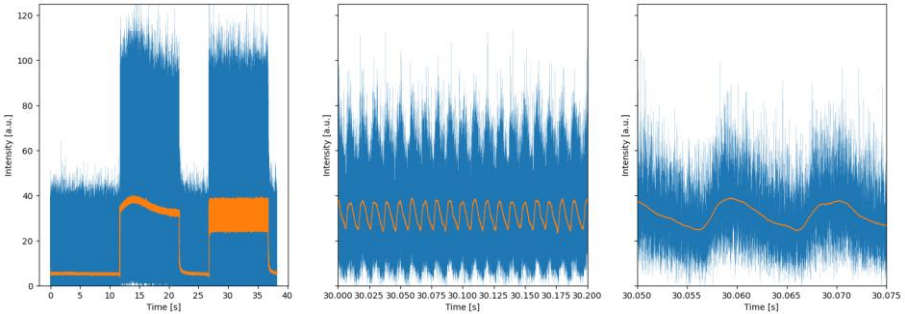

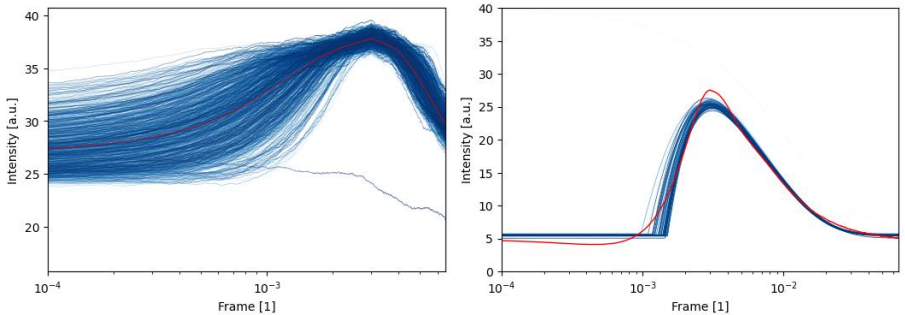

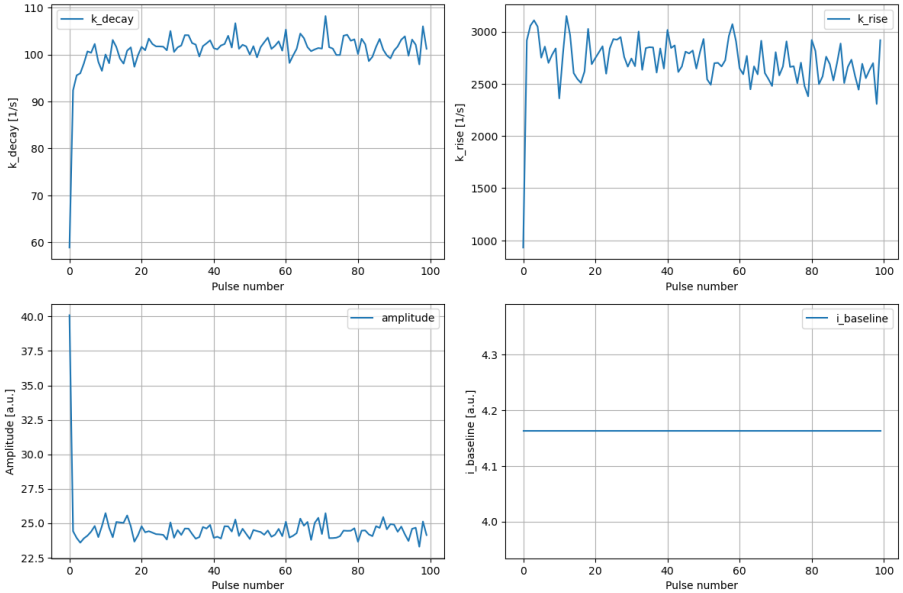

Mean k_decay: 100.93 1/s
Mean k_rise: 2712.23 1/s
Mean amplitude: 24.58 a.u.
Mean i_baseline: 4.16 a.u.